

# Spectroscopic, structural and lifetime calculations of the ground and low-lying excited states of the $\text{BeNa}^+$ , $\text{BeK}^+$ , and $\text{BeRb}^+$ molecular ions

Hela Ladjimi<sup>1</sup>, Mohamed Farjallah<sup>1</sup> and Hamid Berriche<sup>1,2,3</sup> 

<sup>1</sup>Laboratory of Interfaces and Advanced Materials, Faculty of Science, University of Monastir, 5019 Monastir, Tunisia

<sup>2</sup>Department of Mathematics and Natural Sciences, School of Arts and Sciences, American University of Ras Al Khaimah, RAK, PO Box 10021, United Arab Emirates

E-mail: [hamid.berriche@aurak.ac.ae](mailto:hamid.berriche@aurak.ac.ae) and [hamidberriche@yahoo.fr](mailto:hamidberriche@yahoo.fr)

Received 23 December 2019, revised 6 February 2020

Accepted for publication 24 February 2020

Published 16 April 2020



## Abstract

Based on the *ab-initio* approach and using the non-empirical pseudo-potential formalism for  $\text{Be}^{2+}$ ,  $\text{Na}^+$ ,  $\text{K}^+$  and  $\text{Rb}^+$  cores, large Gaussian basis sets and full valence configuration interaction (FCI), alkali-metal atom and the Beryllium ionic pairs are treated as effective two-electron systems. The potential energy curves and their spectroscopic constants for the low-lying excited states of different  $1,3\Sigma^+$ ,  $1,3\Pi$  and  $1,3\Delta$  symmetries of these molecular ions have been performed. In addition to the vibrational properties, permanent and transition dipole moments functions have been also calculated and analyzed. The lifetimes of the vibrational states of the ground state are calculated taking into account the decay rates of the vibrational states in terms of spontaneous emission, and stimulated emission induced by black body radiation. The radiative lifetimes of the vibrational levels of the first  $A^1\Sigma^+$  and second  $C^1\Sigma^+$  excited states are calculated using both ‘*Franck-Condon*’ and ‘*Sum rule*’ approximations. In all studied alkali-metal Beryllium molecular ions the ground states  $X^1\Sigma^+$  have much longer lifetimes than any excited states with an order of second, while an order of nanosecond is found for the first and second excited states,  $A^1\Sigma^+$  and  $C^1\Sigma^+$ .

Supplementary material for this article is available [online](#)

Keywords: potential energy curves, pseudo-potential, dipole moments, *franck-Condon*, ‘*sum rule*’ approximation, radiative lifetimes

(Some figures may appear in colour only in the online journal)

## 1. Introduction

During the past years, the field of laser cooling of neutral atoms [1] and atomic ions [2] has greatly developed, since it has been an essential tool in the development of atomic optics [3], Bose–Einstein condensate [4] and trapped ions [5–7]. In addition, trapped cold ions are a promising candidate in the field of quantum optics and in the implementation of the

quantum computer [8]. Furthermore, the study of cold and ultracold molecular ions has pertinence in diverse areas such as metrology [9, 10], astro-chemistry [11] and it is important for a variety of fundamental studies in physics such as the measure of the electron dipole moment [12].

Because of their interesting energy level scheme the combination between the alkali and alkaline-earth systems are very attractive for both experimental and theoretical research. In fact, many recently experimental works have been performed based on the combinations of alkali atoms and

<sup>3</sup> Author to whom any correspondence should be addressed.

**Table 1.** The calculated dissociation energies and their difference  $|\Delta E|$  with the experimental ones of  $\text{BeNa}^+$  molecular ion.

Asymptotic limit	This work ( $\text{cm}^{-1}$ )	Exp ( $\text{cm}^{-1}$ ) [44]	$ \Delta E $ ( $\text{cm}^{-1}$ )	State
$\text{Be } ({}^1\text{S}(2s^2)) + \text{Na}^+$	-222590.448	-222073.365	517.08	$X^1\Sigma^+$
$\text{Be } ({}^3\text{P}(2s2p)) + \text{Na}^+$	-200490.632	-200095.138	395.49	$1^3\Sigma^+, 1^3\Pi$
$\text{Be}^+ (2s) + \text{Na} (3s)$	-188336.984	-188330.839	6.14	$2^1\Sigma^+, 2^3\Sigma^+$
$\text{Be } ({}^1\text{P}(2s2p)) + \text{Na}^+$	-178998.543	-179506.408	507.86	$3^1\Sigma^+, 1^1\Pi$
$\text{Be}^+ (2s) + \text{Na} (3p)$	-171336.231	-171363.446	27.21	$4^1\Sigma^+, 3^3\Sigma^+, 2^{1,3}\Pi$
$\text{Be } ({}^3\text{S}(2s3s)) + \text{Na}^+$	-169980.973	-169983.168	2.19	$3^3\Sigma^+$
$\text{Be } ({}^1\text{S}(2s3s)) + \text{Na}^+$	-167471.057	-167397.972	73.08	$5^1\Sigma^+$
$\text{Be } ({}^1\text{D}(2p^2)) + \text{Na}^+$	-165146.159	-165192.907	46.75	$6^1\Sigma^+, 3^1\Pi, 1^1\Delta$
$\text{Be } ({}^3\text{P} (2s3p)) + \text{Na}^+$	-163151.131	-163162.105	10.09	$5^3\Sigma^+, 3^3\Pi$

**Table 2.** The calculated dissociation energies and their difference  $|\Delta E|$  with the experimental ones of  $\text{BeK}^+$  molecular ion.

Asymptotic limit	This work( $\text{cm}^{-1}$ )	Exp( $\text{cm}^{-1}$ ) [44]	$ \Delta E $ ( $\text{cm}^{-1}$ )	State
$\text{Be } {}^1\text{S}(2s^2) + \text{K}^+$	-222590.448	-222073.365	517.08	$X^1\Sigma^+$
$\text{Be } ({}^3\text{P}(2s2p)) + \text{K}^+$	-200490.632	-200095.138	395.49	$1^3\Sigma^+, 1^3\Pi$
$\text{Be}^+ (2s) + \text{K} (4s)$	-181896.929	-181891.004	5.92	$2^1\Sigma^+, 2^3\Sigma^+$
$\text{Be } ({}^1\text{P}(2s2p)) + \text{K}^+$	-178998.543	-179506.408	507.86	$3^1\Sigma^+, 1^1\Pi$
$\text{Be } ({}^3\text{S}(2s3s)) + \text{K}^+$	-169980.973	-169983.168	2.19	$3^3\Sigma^+$
$\text{Be}^+ (2s) + \text{K} (4p)$	-168873.941	-168867.357	6.58	$4^1\Sigma^+, 4^3\Sigma^+, 2^{1,3}\Pi$
$\text{Be } ({}^1\text{S}(2s3s)) + \text{K}^+$	-167471.057	-167397.972	73.08	$5^1\Sigma^+$
$\text{Be } ({}^1\text{D}(2p^2)) + \text{K}^+$	-165146.159	-165192.907	46.75	$6^1\Sigma^+, 3^1\Pi, 1^1\Delta$
$\text{Be } ({}^3\text{P} (2s3p)) + \text{K}^+$	-163151.131	-163162.105	10.97	$5^3\Sigma^+, 3^3\Pi$

**Table 3.** The calculated dissociation energies and their difference  $|\Delta E|$  with the experimental ones of  $\text{BeRb}^+$  molecular ion.

Asymptotic limit	This work( $\text{cm}^{-1}$ )	Exp( $\text{cm}^{-1}$ ) [44]	$ \Delta E $ ( $\text{cm}^{-1}$ )	State
$\text{Be } {}^1\text{S}(2s^2) + \text{Rb}^+$	-222590.448	-222073.365	517.08	$X^1\Sigma^+$
$\text{Be } ({}^3\text{P}(2s2p)) + \text{Rb}^+$	-200490.632	-200095.138	395.49	$1^3\Sigma^+, 1^3\Pi$
$\text{Be}^+ (2s) + \text{Rb} (5s)$	-180578.104	-180571.959	6.14	$2^1\Sigma^+, 2^3\Sigma^+$
$\text{Be } ({}^1\text{P}(2s2p)) + \text{Rb}^+$	-178998.543	-179506.408	507.86	$3^1\Sigma^+, 1^1\Pi$
$\text{Be } ({}^3\text{S}(2s3s)) + \text{Rb}^+$	-169980.973	-169983.168	2.19	$3^3\Sigma^+$
$\text{Be}^+ (2s) + \text{Rb} (5p)$	-167840.873	-167834.947	5.92	$4^1\Sigma^+, 4^3\Sigma^+, 2^{1,3}\Pi$
$\text{Be } ({}^1\text{S}(2s3s)) + \text{Rb}^+$	-167471.057	-167397.972	73.08	$5^1\Sigma^+$
$\text{Be } ({}^1\text{D}(2p^2)) + \text{Rb}^+$	-165146.159	-165192.907	46.75	$6^1\Sigma^+, 3^1\Pi, 1^1\Delta$
$\text{Be } ({}^3\text{P} (2s3p)) + \text{Rb}^+$	-163151.131	-163162.105	10.97	$5^3\Sigma^+, 3^3\Pi$

alkaline-earth atomic ions as an optical dipole trap of alkali atoms merged in a Paul trap containing alkaline-earth ions: Rb atoms with  $\text{Ca}^+$  [13, 14] and  $\text{Ba}^+$  [15–17] ions. In addition, collisional cooling of laser precooled  $\text{Ca}^+$  ions by ultracold Na atoms is experimentally performed [18].

In recent times, by using the improved pseudo-potential technique developed by Foucault *et al* [19], many calculations of the electronic structure of the molecular ions systems combining the alkali and alkaline-earth atoms and ions such as  $\text{BeH}^+$  [20],  $\text{BeLi}^+$  [21],  $\text{MgLi}^+$  [22],  $\text{CaH}^+$  [23] and  $\text{SrH}^+$  [24], have been extensively performed. Recently, Szczepkowski *et al* [25] recorded spectral bands for the  $X^2\Sigma^+$  and  $2^2\Sigma^+$  electronic transition in the  $\text{KSr}$  molecule at moderate resolution using the thermoluminescence technique. The spectra were simulated using three kinds of advanced electronic structure calculations, allowing for an assessment of their accuracy on one hand, and for the derivation of fundamental spectroscopic constants of the  $X^2\Sigma^+$   $\text{KSr}$  ground state

and the excited electronic state  $2^2\Sigma^+$ , on the other hand. They used in their simulations FCI + ECP + CPP (effective three-electron system), RCCSD(T) and MRCI calculations. Among the three theoretical approaches, Szczepkowski *et al* found that FCI + ECP + CPP approaches provide the best possible agreement with their experimental measurements.

Recently, Fedorov *et al* [26] executed a theoretical study for the ground electronic state of a variety of ions  $\text{BeLi}^+$ ,  $\text{MgLi}^+$ ,  $\text{BeNa}^+$ , and  $\text{MgNa}^+$ . They used both coupled cluster with singles doubles and triples excitation CCSD(T) and the multireference configuration interaction methods MRCI. Later, they used the obtained results of the ground potential energy curves and the permanent dipole moment to determine and calculate the lifetimes of the ground and excited vibrational states of these ions.

Despite Beryllium being a rare and toxic element, Be-based metal–organic frameworks have been synthesized and characterized [27]. The interactions between neutral and ionic

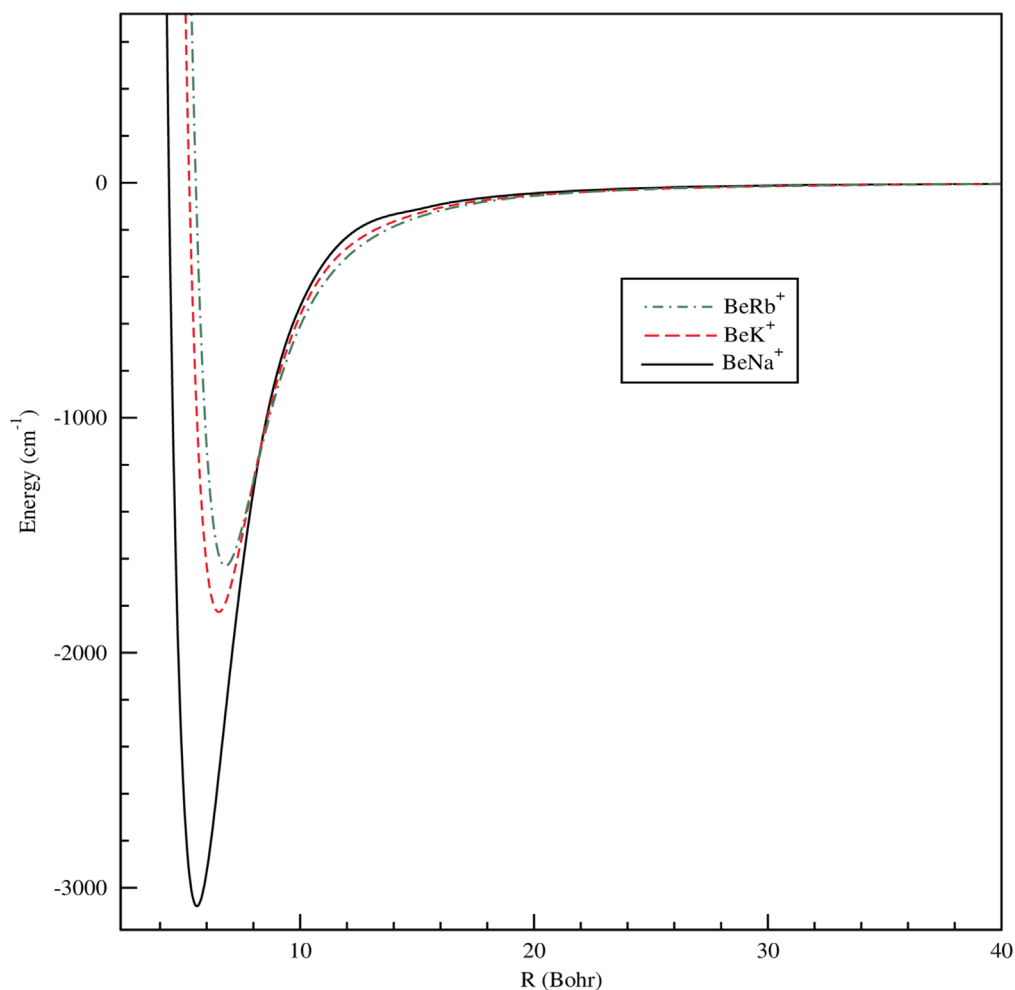


**Figure 1.** Potential energy curves for the ground  $X^1\Sigma^+$  state of  $\text{BeAlk}^+$  ( $\text{Alk} = \text{Na}, \text{K}$  and  $\text{Rb}$ ) molecules with the CIPCI calculation.

Be and alkali atoms are important and can attract research interests on cold molecules. Since  $\text{Be}^+$  ions can be laser-cooled inside of ion traps, the energetic and dynamical properties of the  $\text{BeAlk}^+$  molecular ions are of potential interest in the field of cold molecular ions. In addition, the Beryllium is of interest for astrophysics and astrochemistry [28], and despite its low abundance, the  $\text{Be}^+$  ion is considered as an important astrophysical tracer.

In the present work, an extended theoretical calculation of the low-lying excited electronic states of the  $\text{BeNa}^+$ ,  $\text{BeK}^+$ , and  $\text{BeRb}^+$  is performed. The adiabatic potential energy curves for  $^1,3\Sigma^+$  and  $^1,3\Pi$  symmetries of these molecular systems dissociating into  $\text{Be}(2s^2, 2s2p, 2s3s, 2p^2, 2s3p$  and  $2s3d) + \text{Alk}^+$  ( $\text{Alk} = \text{Na}, \text{K}$  and  $\text{Rb}$ ) and  $\text{Be}^+(2s, 2p, 3s$   $3p$  and  $3d) + \text{Alk}$  ( $\text{Alk} = \text{Na}, \text{K}$  and  $\text{Rb}$ ) are presented. Spectroscopic constants, vibrational spacing, permanent and transition dipole moments are presented and discussed. The vibrational lifetime of the ground  $X^1\Sigma^+$  and the two low lying excited states of symmetry  $^1\Sigma^+$  ( $A^1\Sigma^+$  and  $C^1\Sigma^+$ ) are performed for each system. The calculation of the vibrational lifetime of the  $A^1\Sigma^+$  state is calculated here using two different approximations ‘*Franck-Condon*’ and ‘*sum-rule*’ approximations. This work follows previous studies that

treated the diatomic molecular ion as effective two valence electrons systems: the alkali and alkaline-earth ions [20–22] and alkali dimers [29–36]. This study is a continuation of our previous theoretical work [37], which dealt with only the first three states of  $^1\Sigma^+$  symmetry for each molecular ion  $\text{BeNa}^+$ ,  $\text{BeK}^+$ , and  $\text{BeRb}^+$ . The potential energy curves were used to perform elastic collision at cold temperature to predict the formation of these molecular ionic systems via photo-association. To the best of our knowledge, no experimental nor theoretical studies are available in the literature for the excited states of  $\text{BeAlk}^+$  ( $\text{Alk} = \text{Na}, \text{K}$  and  $\text{Rb}$ ) molecular ionic systems.

This paper is organized as follows: in section 2, we briefly present the computational methods and provide some numerical details. In section 3, which is separated into three parts and it is devoted to present the obtained results; first, we present the adiabatic potential energy curves and the spectroscopic constants for numerous  $^1,3\Sigma^+$ ,  $^1,3\Pi$  and  $^1,3\Delta$  states dissociating into the first nine asymptotic limits for each  $\text{BeAlk}^+$  system. The permanent and transition dipole moments are presented in the second part; while the vibrational analysis and lifetime results are presented in the third part. Finally, we summarize our conclusion in section 4.

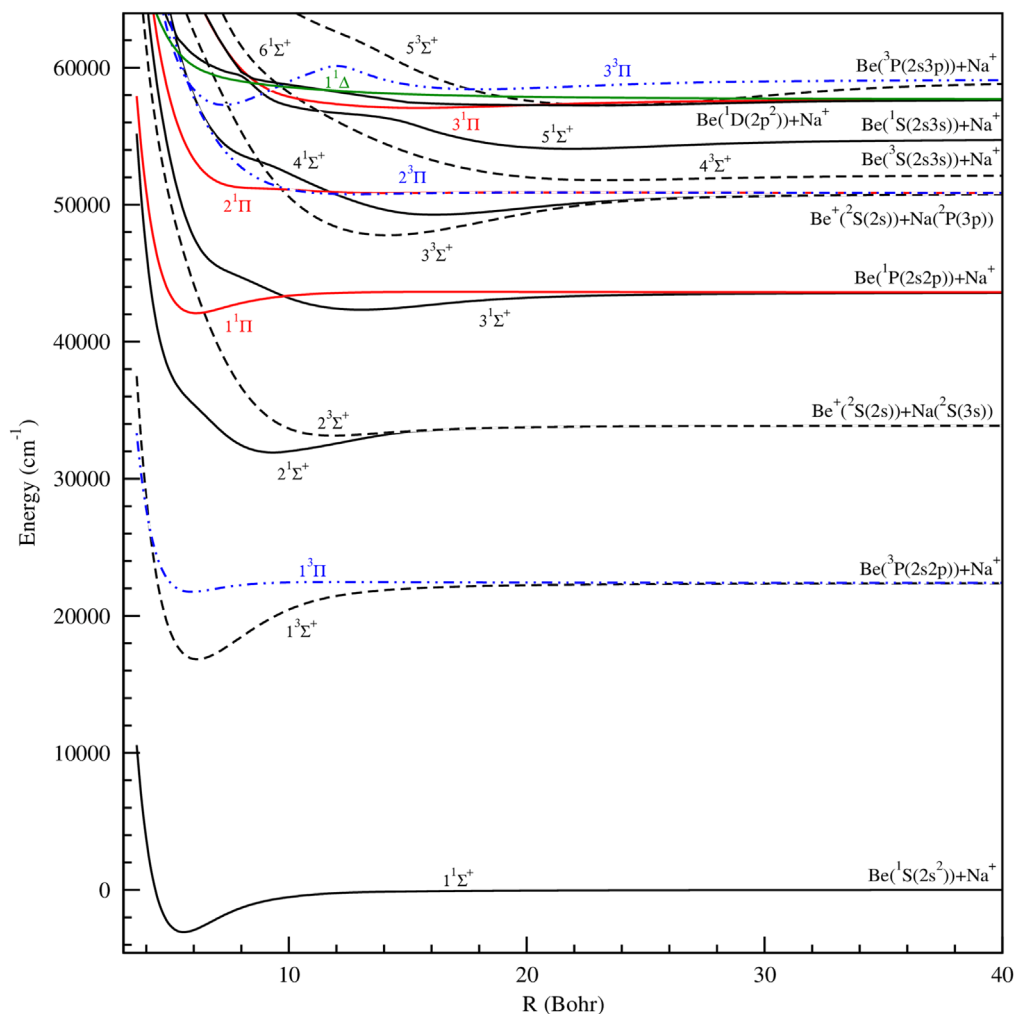


**Figure 2.** Potential energy curves of  $1,3\Sigma^+$ ,  $1,3\Pi$  and  $1\Delta$  states of  $\text{BeNa}^+$  molecular ion.

## 2. Methods of calculation

Complete structure and spectroscopic study is performed here for  $\text{BeAlk}^+$  ( $\text{Alk} = \text{Na}, \text{K}, \text{Rb}$ ) molecular ionic systems using the CIPSI package (Configuration Interaction by Perturbation of a multiconfiguration wave function Selected Iteratively) of the ‘Laboratoire de Physique et Chimie Quantique of Toulouse in France’. The calculation is based on the self-consistent field (SCF) method followed by a full valence configuration interaction (FCI) calculation.

The same quantum chemistry methods have been used in our previous works for the alkaline earth-alkali systems  $\text{BeAlk}^+$  ( $\text{Alk} = \text{H}, \text{Li}$ ) [20, 21]. The  $\text{BeAlk}^+$  ion is treated as a two-electron system using the non-empirical pseudopotential of Barthelat and Durand [38], in its semi-local form used in many previous works [30–36]. This method consists in replacing each core  $\text{Be}^{2+}$  and  $\text{Alk}^+$  by an effective potential. The polarizable cores of  $\text{Be}^{2+}$  and  $\text{Alk}^+$  are replaced by semi-empirical pseudo-potential supplemented by both formula CPP (Core Polarization Potentials) and ECP (Effective Core Potential). This approximation allows us to use large Gaussian basis sets where the aim is to reach accurately more excited molecular states. The core-core and core-valence

correlation corrections have been considered according to the formalism of Müller *et al* [39]. The CPP expression is defined as a function of both  $\alpha_c$  and  $\vec{f}_c$ , which represents respectively the dipole polarizability of the core (c) and the electric field created by the valence electron and all other centers’ cores as represented by this equation:

$$V_{cpp} = -\frac{1}{2} \sum_c \alpha_c \vec{f}_c^2 \quad (1)$$

$$\text{Such as: } \vec{f}_c = \sum_{i \neq c} \frac{\vec{r}_{ci}}{r_{ci}^3} F(r_{ci}, \rho_c^i) - \sum_{c' \neq c} Z_{c'} \frac{\vec{R}_{c'c}}{R_{c'c}^3} \quad (2)$$

$\vec{R}_{c'c}$  is the core-core vector,  $\vec{r}_{ci}$  is the core-electron vector, and  $F_l$  represents the  $l$ -dependent cut-off function explored by Foucault *et al* [40].

$$F_l = \left[ l - \exp\left(-\frac{r_{ci}^2}{\rho_c^2}\right) \right] \quad (3)$$

In this work we used Gaussian-type orbital basis sets, (7s9p10d/7s8p9d) [20, 21], (7s6p5d3f/6s5p4d2f) [41], (7s5p7d1f/6s5p5d1f) [42] and (7s4p5d1f/6s4p4d1f) [43] respectively for the Beryllium, Sodium, Potassium and Rubidium atoms. The use of these basis sets allowed us to reproduce the atomic states  $2s$ ,  $2p$ ,  $3s$ ,  $3p$  and  $3d$  for  $\text{Be}^+$ ;  $2s^2$ ,

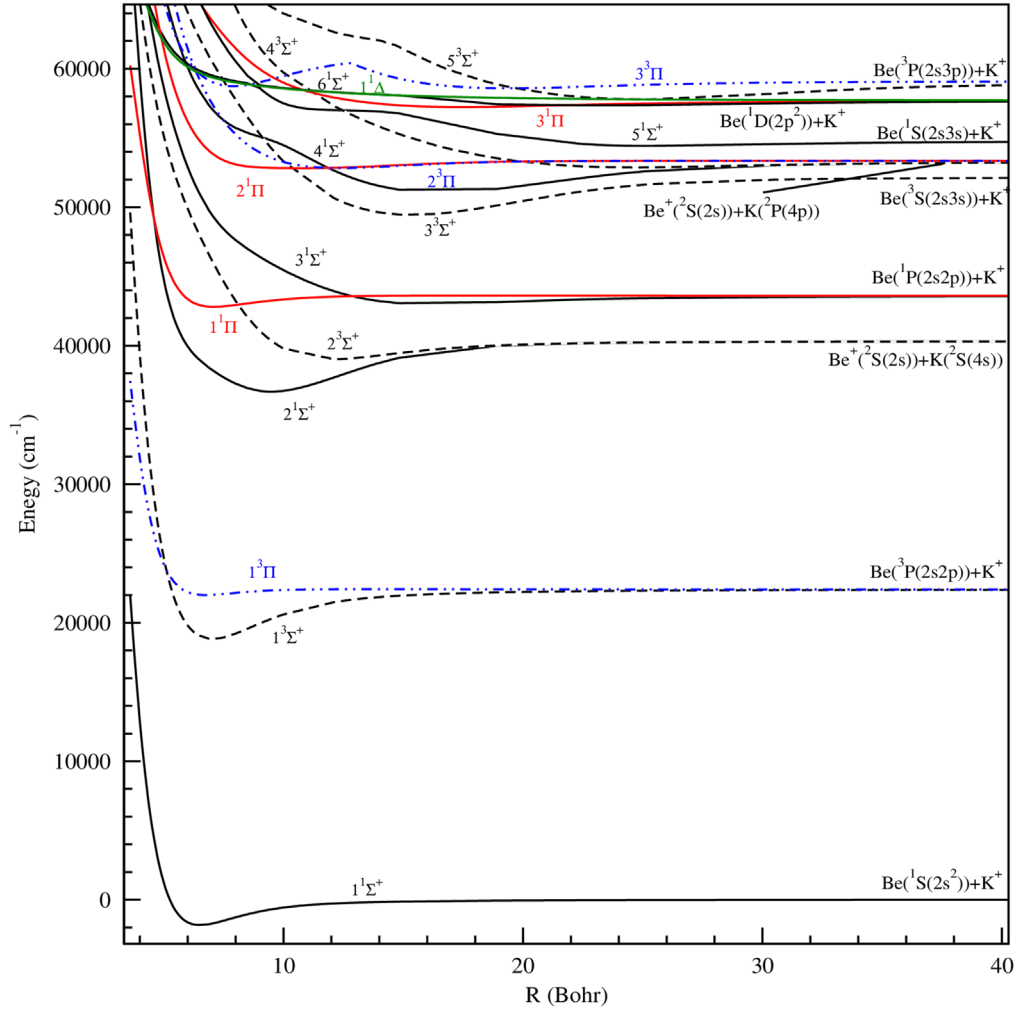


**Figure 3.** Potential energy curves of  $^{1,3}\Sigma^+$ ,  $^{1,3}\Pi$  and  $^1\Delta$  states of  $\text{BeK}^+$  molecular ion.

$2s2p$ ,  $2s3s$ ,  $2p^2$ ,  $2s3p$  and  $2s3d$  for Be;  $3s$ ,  $3p$ ,  $4s$ ,  $3d$ ,  $4p$ ,  $5s$ , and  $4d$  for Na;  $4s$ ,  $4p$ ,  $5s$ ,  $3d$ ,  $5p$ ,  $4d$ , and  $6s$  for K;  $5s$ ,  $5p$ ,  $4d$ ,  $6s$ ,  $6p$ ,  $5d$  and  $7s$  for Rb. In the present work, the core polarizabilities are taken to be  $\alpha_{\text{Be}^{2+}} = 0.0519 a_0^3$ ,  $\alpha_{\text{Na}^+} = 0.99^3 a_0^3$ ,  $\alpha_{\text{K}^+} = 5.354 a_0^3$ , and  $\alpha_{\text{Rb}^+} = 9.245 a_0^3$  [39]. The used cut-off parameters for the lowest valence  $s$ ,  $p$  and  $d$  one-electron states of the Na, K, Rb and Be atoms are represented in [37]. The first nine molecular asymptotic energies for the  $\text{BeNa}^+$ ,  $\text{BeK}^+$  and  $\text{BeRb}^+$  related to the electronic states of different symmetries  $^{1,3}\Sigma^+$ ,  $^{1,3}\Pi$  and  $^{1,3}\Delta$  are illustrated respectively in tables 1–3. From these tables, we can conclude that our dissociation energies are in good agreement with the experimental results [44]. The accuracy of our calculation at the atomic levels will be transferred to the molecular calculation represented in the next part of this paper.

The methodology, used in this work, for calculating of the vibrational lifetimes of the ground state  $X^1\Sigma^+$  is described as below:

$$\tau_i^{-1} = \sum_{f < i} A_{if} + \sum_f B_{if} \quad (5)$$

The first term  $A_{if}$  is the Einstein coefficient describing the probability of spontaneous emission from the vibrational state  $i$  to the lower energy state  $f$ :

$$A_{if} = \frac{4\omega_{if}^3}{3C^3} |i|\mu(R)|f|^2 \quad (6)$$

$\omega_{if} = |E_f - E_i|$  is the transition frequency between the two states  $i$  and  $f$ , and  $\mu(R)$  is the permanent dipole moment of the ground state  $X^1\Sigma^+$ .

The second term is related to the Black Body Radiation (BBR), which is coming from the surrounding environment at  $T = 300$  K, and it can induce stimulated absorption and emission processes, which are described by the Einstein coefficient  $B_{if} = A_{if} N(\omega_{if})$ , where the number of black body photons is given by:

$$N(\omega_{if}) = \left( \exp\left(\frac{\omega_{if}}{k_B T}\right) - 1 \right)^{-1} \quad (7)$$

The calculation of the vibrational lifetimes of the excited states takes into account two possible transitions: *bound-bound* and *bound-free* transitions.

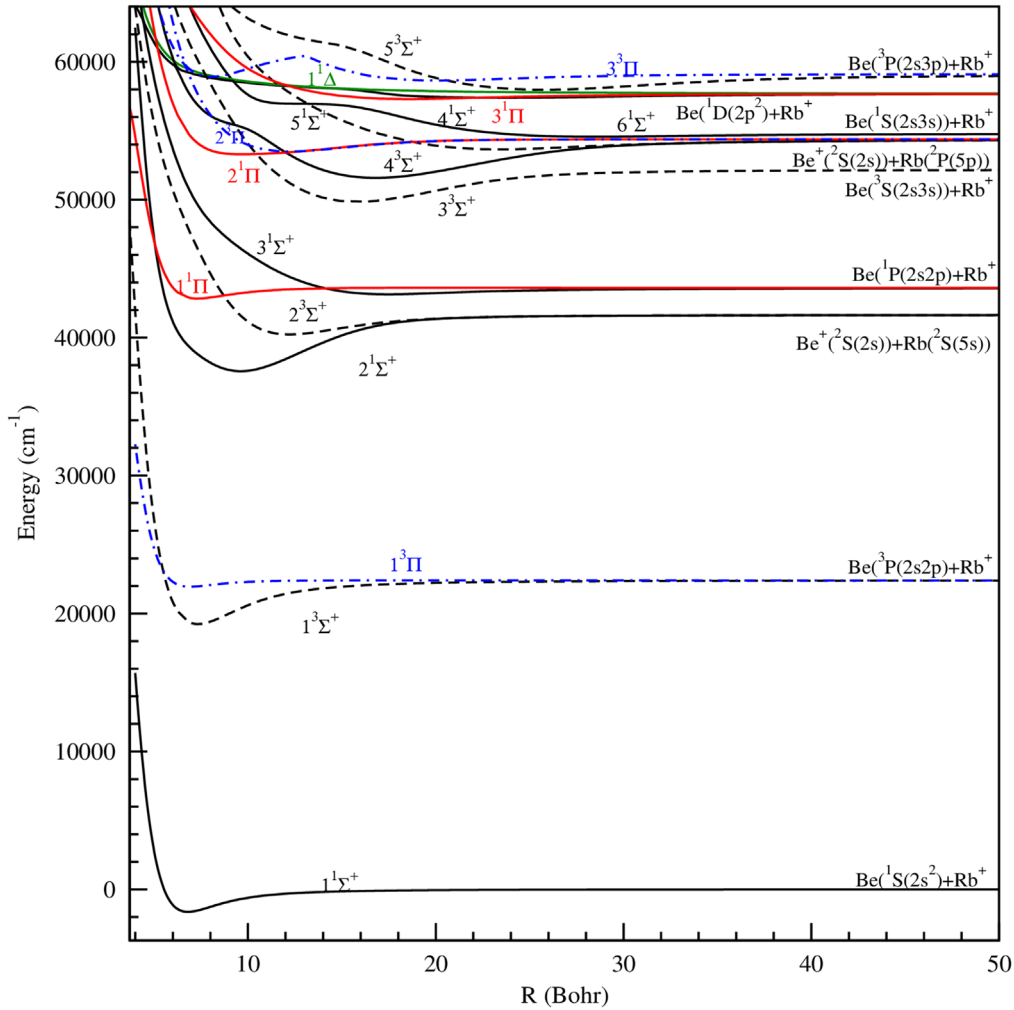


**Figure 4.** Potential energy curves of  $1,3\Sigma^+$ ,  $1,3\Pi$  and  $1\Delta$  states of  $\text{BeRb}^+$  molecular ion.

The radiative lifetime of a vibrational level  $v'$  corresponding to only *bound-bound* transitions is given by:

$$\tau_{v'} = \frac{1}{\Gamma_{v'}}, \quad \Gamma_{v'} = \sum_{v=0}^{nv'} A_{vv'} \quad (8)$$

$A_{vv'}$  is the Einstein coefficient taking for example the transition between  $A^1\Sigma^+(v')$  and  $X^1\Sigma^+(v)$  levels states.

It has been shown previously, by Zemke *et al* [45], that there is a missing contribution in the radiative lifetimes. It corresponds to the *bound-free* transitions, which is more significant for the higher vibrational levels close to the dissociation limit of the excited electronic states, which are found in the form of the continuum radiation to states above the dissociation limit of the ground state. It matches the contribution of the *bound-free* transition missed in the equation (8). It is related to the transition between the vibrational level  $v'$ , which belongs to the excited electronic state to the continuum of the ground state or the lower state in general. Such contribution is not negligible as it was demonstrated by Zemke *et al* [45], Partridge *et al* [46], and Berriche *et al* [47]. This term is more obvious for the higher vibrational levels due the difference in location of the

potential wells. This contribution is calculated using two different approximations: 'Franck-Condon' [46, 47] and 'sum rule' [48, 49] approach.

### 2.1. 'Franck-Condon' approximation

This approximation, which was proposed by Zemke *et al* [45], gives the bound-free contribution as:

$$A_{v'}(\text{bound} - \text{free}) = \frac{64\pi^2}{3h^4c^3} |\mu(R_{v'+})|^2 FC_{v',cont} (\Delta E)_{v',cont}^3 \quad (9)$$

Where  $\Delta E_{v',cont} = E_{v'} - E_{as}$  is the energy difference between the vibrational level  $v'$  and the energy of the asymptotic limit of the lower electronic state, to which belongs the continuum. The quantity  $\mu(R_{v'+})$  corresponds to the transition dipole moment at the right external turning point of the vibrational level  $v'$ .

$$FC_{v',cont} = \int |\chi_{v'}| \chi_E|^2 dE = 1 - \sum_{v=0}^{nv'} |\chi_{v'}| \chi_v|^2 \quad (10)$$

**Table 4.** Spectroscopic constants of the ground and excited singlet and triplet electronic states of BeNa<sup>+</sup> molecular ion.

State	R <sub>e</sub> (Bohr)	D <sub>e</sub> (cm <sup>-1</sup> )	T <sub>e</sub> (cm <sup>-1</sup> )	ω <sub>e</sub> (cm <sup>-1</sup> )	ω <sub>e</sub> χ <sub>e</sub> (cm <sup>-1</sup> )	B <sub>e</sub> (cm <sup>-1</sup> )	References
X <sup>1</sup> Σ <sup>+</sup>	5.580	3079	0	200.33	3.25	0.299203	[37] <sup>a</sup>
	5.686		0	202			[50] <sup>a</sup>
	5.731		0	199			[50] <sup>b</sup>
	5.624	3064.7	0	199	3.2		[26] <sup>a</sup>
	5.617	3018.80	0	193	1.9		[26] <sup>b</sup>
	5.614	3085.2	0	194.6	1.9		[26] <sup>c</sup>
2 <sup>1</sup> Σ <sup>+</sup>	9.33	1961	34998	93.06	1.48	0.107130	[37] <sup>a</sup>
3 <sup>1</sup> Σ <sup>+</sup>	12.92	1298	45378	53.00	0.38	0.055720	[37] <sup>a</sup>
4 <sup>1</sup> Σ <sup>+</sup>	16.14	1569	52357	45.11	0.19	0.035691	This work
5 <sup>1</sup> Σ <sup>+</sup>	21.88	700	57164	29.82	0.38	0.019414	This work
6 <sup>1</sup> Σ <sup>+</sup>	12.12	1242*					This work
1 <sup>3</sup> Σ <sup>+</sup>	6.15	5572	19908	189.35	1.78	0.246133	This work
2 <sup>3</sup> Σ <sup>+</sup>	11.87	729	36230	56.08	1.08	0.065993	This work
3 <sup>3</sup> Σ <sup>+</sup>	14.13	3077	50849	61.99	0.20	0.046598	This work
4 <sup>3</sup> Σ <sup>+</sup>	23.31	383	54870	22.58	0.27	0.017119	This work
5 <sup>3</sup> Σ <sup>+</sup>	23.40	1847	60331	30.97	0.07	0.016978	This work
1 <sup>1</sup> Π	6.11	1519	45160	148.82	3.78	0.249279	This work
2 <sup>1</sup> Π	14.13	41*					This work
3 <sup>1</sup> Π	15.43	620	60140	26.09	0.23	0.039076	This work
1 <sup>3</sup> Π	5.92	651	24830	125.44	4.47	0.265214	This work
2 <sup>3</sup> Π	12.78	85	53846	27.59	0.96	0.056913	This work
3 <sup>3</sup> Π	7.27	1817	60366	132.98	0.84	0.171688	This work
	18.01	674	61509	28.95	0.31	0.028675	This work
1 <sup>1</sup> Δ	Repulsive						This work

**Table 5.** Spectroscopic constants of the ground and excited singlet and triplet electronic states of BeK<sup>+</sup> molecular ion.

States	R <sub>e</sub> (Bohr)	D <sub>e</sub> (cm <sup>-1</sup> )	T <sub>e</sub> (cm <sup>-1</sup> )	ω <sub>e</sub> (cm <sup>-1</sup> )	ω <sub>e</sub> χ <sub>e</sub> (cm <sup>-1</sup> )	B <sub>e</sub> (cm <sup>-1</sup> )	References
X <sup>1</sup> Σ <sup>+</sup>	6.52	1833	0	135.61	2.96	0.193599	[37] <sup>a</sup>
2 <sup>1</sup> Σ <sup>+</sup>	9.48	3638	38515	88.06	0.53	0.091501	[37] <sup>a</sup>
3 <sup>1</sup> Σ <sup>+</sup>	16.12	593	44838	33.52	0.47	0.031589	[37] <sup>a</sup>
4 <sup>1</sup> Σ <sup>+</sup>	16.56	2262	52871	44.83	0.97	0.029977	This work
5 <sup>1</sup> Σ <sup>+</sup>	25.18	364	56253	19.16	0.21	0.012968	This work
6 <sup>1</sup> Σ <sup>+</sup>	Repulsive						This work
1 <sup>3</sup> Σ <sup>+</sup>	7.03	3570	20864	139.38	1.36	0.166269	This work
2 <sup>3</sup> Σ <sup>+</sup>	12.04	1295	40858	61.86	0.47	0.056671	This work
3 <sup>3</sup> Σ <sup>+</sup>	15.38	2745	51262	52.98	0.44	0.034731	This work
4 <sup>3</sup> Σ <sup>+</sup>	24.82	452	54681	20.04	0.22	0.013347	This work
5 <sup>3</sup> Σ <sup>+</sup>	24.94	1316	59606	27.66	0.08	0.013223	This work
1 <sup>1</sup> Π	7.08	795	44638	90.91	2.27	0.164161	This work
2 <sup>1</sup> Π	11.03	516	54623	22.22	0.52	0.067597	This work
3 <sup>1</sup> Π	17.37	459	59064	20.40	0.18	0.027233	This work
1 <sup>3</sup> Π	6.75	406	23829	85.81	6.18	0.179980	This work
2 <sup>3</sup> Π	12.36	524	54615	39.65	1.47	0.053838	This work
3 <sup>3</sup> Π	7.88	363	60571	103.34	1.36	0.132484	This work
	19.41	512	60417	24.53	0.29	0.021865	This work
1 <sup>1</sup> Δ	Repulsive						This work

**Table 6.** Spectroscopic constants of the ground and excited singlet and triplet electronic states of BeRb<sup>+</sup> molecular ion.

Etats	R <sub>e</sub> (Bohr)	D <sub>e</sub> (cm <sup>-1</sup> )	T <sub>e</sub> (cm <sup>-1</sup> )	ω <sub>e</sub> (cm <sup>-1</sup> )	ω <sub>e</sub> χ <sub>e</sub> (cm <sup>-1</sup> )	B <sub>e</sub> (cm <sup>-1</sup> )	References
X <sup>1</sup> Σ <sup>+</sup>	6.81	1630	0	119.74	2.50	0.159460	[37] <sup>a</sup>
2 <sup>1</sup> Σ <sup>+</sup>	9.61	4072	39198	80.53	0.39	0.079968	[37] <sup>a</sup>
3 <sup>1</sup> Σ <sup>+</sup>	17.07	466	44764	25.98	0.36	0.025346	[37] <sup>a</sup>
4 <sup>1</sup> Σ <sup>+</sup>	16.91	2778	53228	41.58	0.17	0.025813	This work
5 <sup>1</sup> Σ <sup>+</sup>	28.46	214	56201	14.98	6.93	0.009072	This work
6 <sup>1</sup> Σ <sup>+</sup>	Repulsive						This work
1 <sup>3</sup> Σ <sup>+</sup>	7.33	3167	20864	121.94	1.52	0.137420	This work
2 <sup>3</sup> Σ <sup>+</sup>	12.21	1407	41862	57.27	0.02	0.049539	This work
3 <sup>3</sup> Σ <sup>+</sup>	15.82	2323	51483	47.77	0.42	0.029499	This work
4 <sup>3</sup> Σ <sup>+</sup>	23.36	720	55286	24.04	0.55	0.013531	This work
5 <sup>3</sup> Σ <sup>+</sup>	25.75	1120	59611	23.22	0.10	0.011142	This work
1 <sup>1</sup> Π	7.30	764	44470	90.91	2.27	0.164161	This work
2 <sup>1</sup> Π	9.71	1090	54930	34.40	3.21	0.078618	This work
3 <sup>1</sup> Π	18.53	384	58936	19.07	0.72	0.021480	This work
1 <sup>3</sup> Π	6.94	456	23577	79.91	5.30	0.179980	This work
2 <sup>3</sup> Π	12.23	881	55134	41.07	1.47	0.049395	This work
3 <sup>3</sup> Π	8.07	176	60558	89.31	0.57	0.113278	This work
	20.08	453	60281	22.16	0.27	0.018333	This work
1 <sup>1</sup> Δ	Repulsive						This work

The (\*) sign denotes the potential barrier.

[26]<sup>a</sup> MOLOPRO:CCSDT/cc-pCVQZ.

[26]<sup>b</sup> MOLOPRO: MRCI/cc-pCVQZ.

[26]<sup>c</sup> MOLPRO: MRCI/aug-cc-pCV5.

[37]<sup>a</sup> CIPCI package.

[50]<sup>a</sup> Gaussian : MP2/6-31G\*□

[50]<sup>b</sup> Gaussian:HF/6-31G\*□

## 2.2. 'Sum rule' approximation

Pazyuk *et al* [48, 49] have implemented this approach. It allows reproducing the radiative lifetime components for diatomic vibronic states. In addition, this approximation has a high efficiency for non-diagonal systems and particularly for those with significant continuum contributions. The radiative lifetime using the approximate sum rule is given by:

$$\frac{1}{\tau} = \int_{R_{\min}}^{R_{\max}} \varphi_{v'}(R) D(r)^2 \Delta U(R)^3 \varphi_{v'}(R) dR \quad (11)$$

$\varphi_{v'}(R)$  is the wave function of the vibrational level belonging to the A<sup>1</sup>Σ<sup>+</sup> excited electronic state. D(R) is the transition dipole moment between the ground X<sup>1</sup>Σ<sup>+</sup> and first excited state A<sup>1</sup>Σ<sup>+</sup>. ΔU(R) is the energy difference between the ground X<sup>1</sup>Σ<sup>+</sup> state and first excited state A<sup>1</sup>Σ<sup>+</sup>.

## 3. Results and discussion

### 3.1. Adiabatic potential energy and spectroscopic constants

Effective Core Polarization ECP and Core-Polarization Potential CPP approach can describe accurately the electronic structure with few-active-electron. Its main advantage is the possibility to investigate the ground and the highly excited molecular states properties with similar accuracy. In this

study, using the ECP + CPP approach and FCI methods, we have determined the adiabatic potential energy curves of three ground states and 49 excited states of <sup>1,3</sup>Σ<sup>+</sup>, <sup>1,3</sup>Π and <sup>1,3</sup>Δ symmetries. They are dissociating into the first 9 dissociations limits Be (2s<sup>2</sup>, 2s2p, 2s3s, 2p<sup>2</sup> and 2s3p) + Alk<sup>+</sup> (Alk = Na, K and Rb) and Be<sup>+</sup>(2s) + Alk (Alk = Na (3s, 3p), K(4s, 4p) and Rb(5s, 5p)) (see tables 1–3) for the BeNa<sup>+</sup>, BeK<sup>+</sup> and BeRb<sup>+</sup> molecular ions. The adiabatic potential energy is performed for a large and dense grid of intermolecular distances from 3.6 to 200.00 Bohr. We report in figure 1 the potential energy curves of the ground states X<sup>1</sup>Σ<sup>+</sup> (defined also as 1<sup>1</sup>Σ<sup>+</sup>) of the BeAlk<sup>+</sup> ionic systems (Alk = Na, K and Rb) using *ab-initio* calculation methods: CIPCI.

As represented in figure 1, the shape of potential energy curves of the ground state X<sup>1</sup>Σ<sup>+</sup> depends on the size and the electronic structure of the alkaline atoms. Indeed, the equilibrium positions obviously increase from BeNa<sup>+</sup> to BeRb<sup>+</sup>. However, the depths of the corresponding wells decrease from Na to Rb and the ground state X<sup>1</sup>Σ<sup>+</sup> behaves more and more like a van der Waals molecules. At large distances, the ground state X<sup>1</sup>Σ<sup>+</sup> for each system are tend to the same dissociation limits correlated to two closed-shell systems Be (2S) and Alk<sup>+</sup> (Alk = Na, K and Rb).

In addition, the potential energy curves for the ground and low-lying excited states of different symmetries, <sup>1,3</sup>Σ<sup>+</sup>, <sup>1,3</sup>Π and

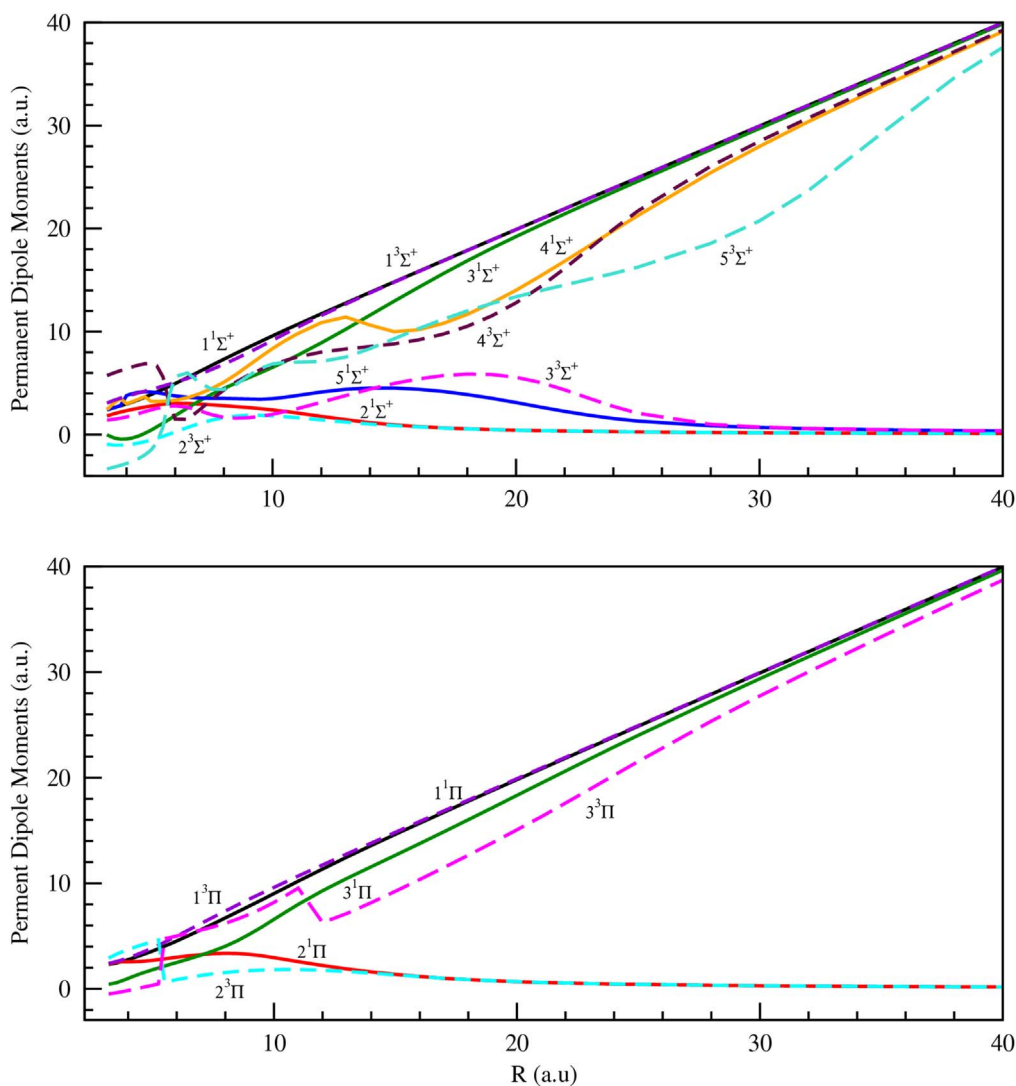


**Figure 5.** Permanent dipole moment of the  $1,3\Sigma^+$  and  $1,3\Pi$  electronic states of  $\text{BeNa}^+$  molecular ion.

$1,3\Delta$  respectively, of  $\text{BeNa}^+$ ,  $\text{BeK}^+$  and  $\text{BeRb}^+$  molecular ions are displayed in figures 2–4.

It is obvious that the ground state,  $X^1\Sigma^+$ , is well separated from the highest excited states correlated to two closed-shell systems  $\text{Be}(^2S)$  and  $\text{Alk}^+$  ( $\text{Alk} = \text{Na}, \text{K}$  and  $\text{Rb}$ ). The second asymptotic limit is the combination of the second atomic excited state of the  $\text{Be}(^3P(2s2p))$  atom and the  $\text{Alk}^+$  alkali ion ( $\text{Alk} = \text{Na}, \text{K}$ , and  $\text{Rb}$ ) with a closed-shell that generates two states  $1^3\Sigma^+$  and  $1^3\Pi$ . Therefore, the energy gap between the ground state dissociation limit and that of the  $1^3\Sigma^+$  and  $1^3\Pi$  states is constant for all  $\text{BeAlk}^+$  ionic systems ( $\text{Alk} = \text{Na}, \text{K}$ , and  $\text{Rb}$ ). It has an order of  $21978\text{ cm}^{-1}$  corresponding to the atomic energy difference between  $\text{Be}(^1S(2s^2))$  and  $\text{Be}(^3P(2s2p))$  states. Note that the  $1^3\Sigma^+$  state is notably attractive and more specifically in the case of the  $\text{BeNa}^+$  molecule, since it has the deepest well  $D_e = 5572\text{ cm}^{-1}$  located at an equilibrium distance  $R_e = 6.15$  Bohr. So the ionic molecule  $\text{BeNa}^+$  is the most stable in its  $1^3\Sigma^+$  state compared to other  $\text{BeAlk}^+$  systems ( $\text{Alk} = \text{K}$ , and  $\text{Rb}$ ). In addition, the well depth of the

considered state decreases with the size of the alkali atom, with  $D_e = 3570, 3167\text{ cm}^{-1}$  respectively for  $\text{BeK}^+$  and  $\text{BeRb}^+$ .

Also, the third dissociation limit of the  $\text{BeAlk}^+$  ion systems ( $\text{Alk} = \text{Na}, \text{K}$  and  $\text{Rb}$ ) is the combination of the ground state of a neutral alkali atom ( $\text{Na}, \text{K}, \text{Rb}$ ) and the  $\text{Be}^+(2s)$  ion, where a valence electron is attached to each atomic partner, giving rise to  $2^1\Sigma^+$  and  $2^3\Sigma^+$  states. The energy difference between the ground state  $1^1\Sigma^+$  (also called state  $X^1\Sigma^+$ ) and the first excited state  $2^1\Sigma^+$  (also called state  $A^1\Sigma^+$ ) increases from  $\text{BeNa}^+$  to  $\text{BeRb}^+$ . Consequently, the ground state is less and less repelled by the  $2^1\Sigma^+$  state. Consequently, it behaves more and more like a van der Waals molecule. In addition, the  $2^1\Sigma^+$  state is clearly deep (several thousand of  $\text{cm}^{-1}$ ) compared to other states of different symmetry. Indeed, the long-range attraction of the charge-induced dipole (varying as  $R^{-4}$ , where  $R$  is the internuclear distance) between  $\text{Be}^+$  and the alkali atom is strong. As the static dipolar polarizability increases with the mass of the alkali atom, the well depths of both the  $2^1\Sigma^+$  and  $2^3\Sigma^+$  states also increase as from  $\text{BeNa}^+$  to  $\text{BeRb}^+$ .

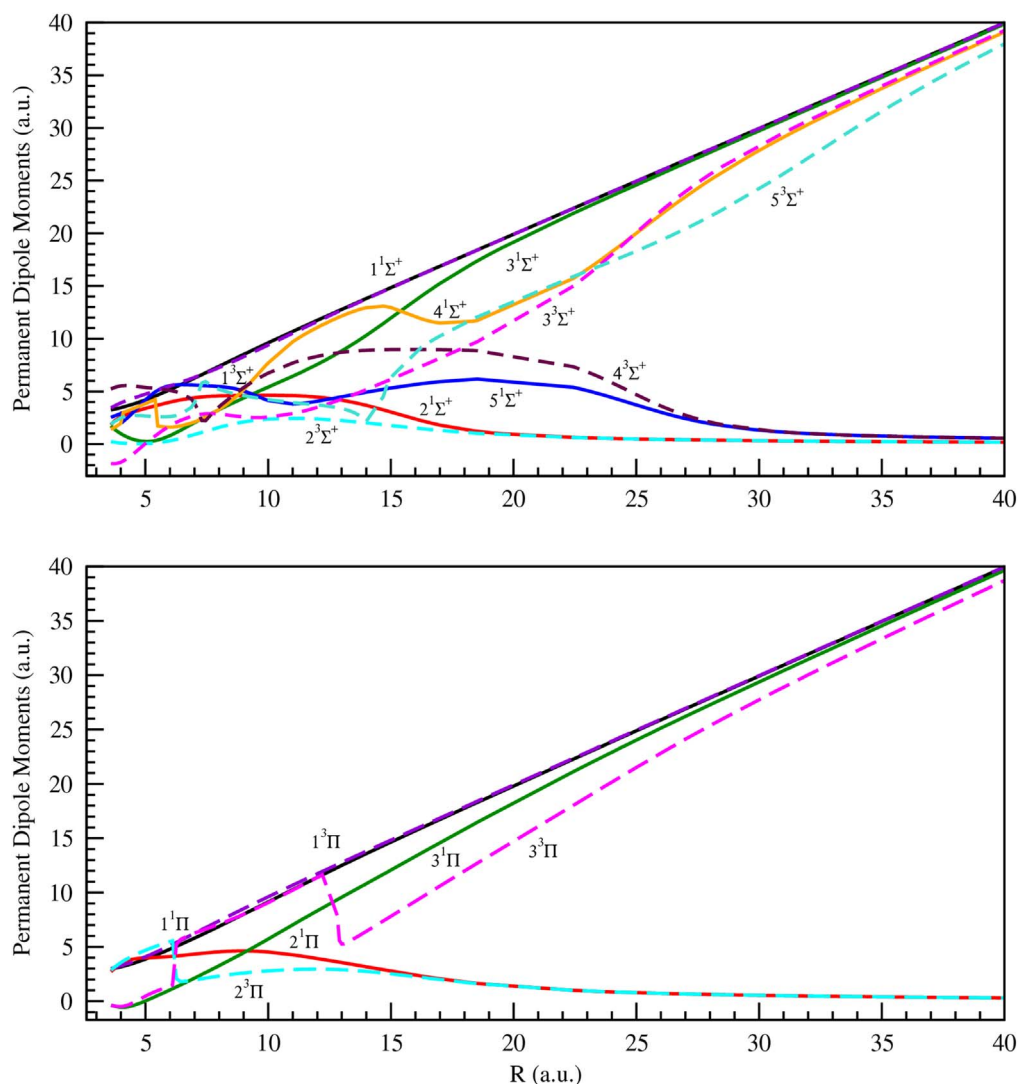


**Figure 6.** Permanent dipole moment of the  $1,3\Sigma^+$  and  $1,3\Pi$  electronic states of  $\text{BeK}^+$  molecular ion.

An interesting behavior is observed for the adiabatic potential energy curves for the highly excited electronic states for different symmetries  $1,3\Sigma^+$  and  $1,3\Pi$ . It corresponds to the presence of the spectacular undulations including multiple barriers and wells. These undulations are related to avoided crossings. Most of them can be explained by the interaction between the adiabatic potential energy curves of different  $\text{Be}^+\text{Alk}$  and  $\text{BeAlk}^+$  structures. For our best knowledge, theoretical spectroscopic information for  $\text{BeNa}^+$ ,  $\text{BeK}^+$  and  $\text{BeRb}^+$  is still limited, except for the ground state ( $X^1\Sigma^+$ ) of the  $\text{BeNa}^+$  ionic molecule. The latter was explored earlier by Pyykkö [50] and recently by Fedorov *et al* [26]. The good agreement for the ground state of  $\text{BeNa}^+$  with that of Pyykkö [50] and Fedorov *et al* [26], encouraged us to deeply investigate the spectroscopic properties of the excited states and to achieve the first complete exploration of the electronic structure of  $\text{BeNa}^+$ ,  $\text{BeK}^+$  and  $\text{BeRb}^+$ . In our previous study [37], we provided only the ground and the two first excited states of symmetry  $1^1\Sigma^+$  for these molecular ionic systems used for elastic scattering and photassociation studies.

All the remaining excited states of  $1,3\Sigma^+$ ,  $1,3\Pi$  and  $1,3\Delta$  symmetries are represented here for the first time. The spectroscopic constants are extracted from the numerical calculated potential energy curves; equilibrium distance ( $R_e$ ), well depth ( $D_e$ ), vertical transition energy ( $T_e$ ), harmonicity frequency ( $\omega_e$ ), anharmonicity frequency ( $\omega_e\chi_e$ ) and the rotational constant ( $B_e$ ). The spectroscopic constants for the ground and the low-lying states of different symmetries are extensively presented in tables 4–6 for  $\text{BeNa}^+$ ,  $\text{BeK}^+$  and  $\text{BeRb}^+$ .

An accurate analysis of these results shows that the most strongly bound states are  $1^3\Sigma^+$  for the  $\text{BeNa}^+$  with depth of well equal to  $5572\text{ cm}^{-1}$ , and the first excited state  $2^1\Sigma^+$  for both  $\text{BeK}^+$  and  $\text{BeRb}^+$  molecular systems with well depths of  $3638$  and  $4072\text{ cm}^{-1}$ , respectively. The  $1,3\Pi$  states are weakly bound with small attractive wells and barriers for all systems, except the  $3^3\Pi$  state for the  $\text{BeNa}^+$ , which has a relatively deep well of  $1817\text{ cm}^{-1}$  located at  $7.27$  Bohr. In addition, we found that the states corresponding to the  $1,3\Delta$  symmetries are all repulsive. Therefore, these cationic

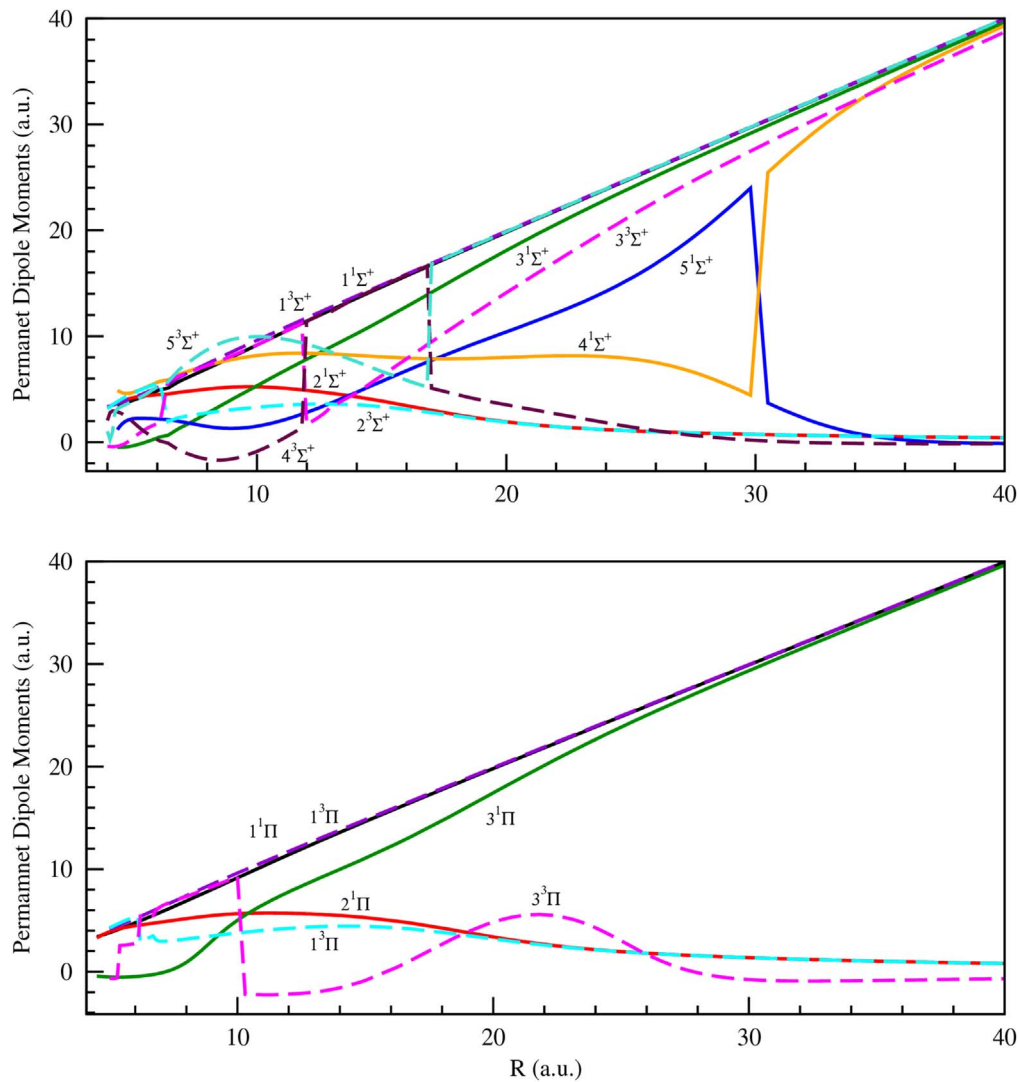


**Figure 7.** Permanent dipole moment of the  $1-3\Sigma^+$  and  $1-3\Pi$  electronic states of  $\text{BeRb}^+$  molecular ion.

molecular systems are considered unstable in the states of symmetries  $1,3\Delta$ .

### 3.2. Permanent and transition dipole moments curves

The formation of cold and ultracold samples of dipolar molecules is currently a challenge for the experiments, which needs accurate information about the electronic properties of the choosing molecule. The permanent and transition dipole moments, represent an appropriate test for assessing the validity and accuracy of *ab-initio* calculations. For instance, the rovibrational cold molecular ions [51, 52], are controlled by the permanent and transition dipole moments (PDM) of the relevant molecular state. Fedorov *et al* [26] published the only available study on dipole moment for the  $\text{BeNa}^+$  ionic molecule. They only calculated the permanent dipole moment for the ground state  $X^1\Sigma^+$ , using CCSD(T) and MRCISD methods with cc-pCVQZ and aug-cc-pCVQZ basis sets. The comparison proves patently that the feature of their permanent dipole moment is very similar to ours. We notice that the implementation of the core polarization in our calculation

decreases in the absolute value the dipole moment compared with the results of Fedorov *et al* [26]. To understand the structure of the ground and excited electronic states, we have evaluated the permanent dipole moments for a large and dense grid of interaction distances from 3.6 to 200 Bohr for all electronic states of  $\text{BeNa}^+$ ,  $\text{BeK}^+$  and  $\text{BeRb}^+$ . Except the results obtained by Fedorov *et al* [26] for  $\text{BeNa}^+$  ground state, the permanent dipole moments of different states for these three systems are represented here for the first time. Figure 5–7 present the permanent dipole moments for the electronic states of  $(1-5)^1\Sigma^+$ ,  $(1-5)^3\Sigma^+$ ,  $(1-3)^1\Pi$ , and  $(1-3)^3\Pi$  states, for  $\text{BeNa}^+$ ,  $\text{BeK}^+$  and  $\text{BeRb}^+$ , respectively. Depending on the interatomic axis orientation, the permanent dipole moments are computed in this work with respect of the same origin. The  $\text{Be}^{2+}$  core is placed at the origin and the Na, K and Rb cores are placed at distance  $R$ .

We remark that the permanent dipole moments of  $^1\Sigma^+$ ,  $^3\Sigma^+$ ,  $^1\Pi$  and  $^3\Pi$  electronic states present at small internuclear distance many abrupt changes. They correspond to the avoided crossings between neighbouring states related to the charge transfer process between the two ionic systems

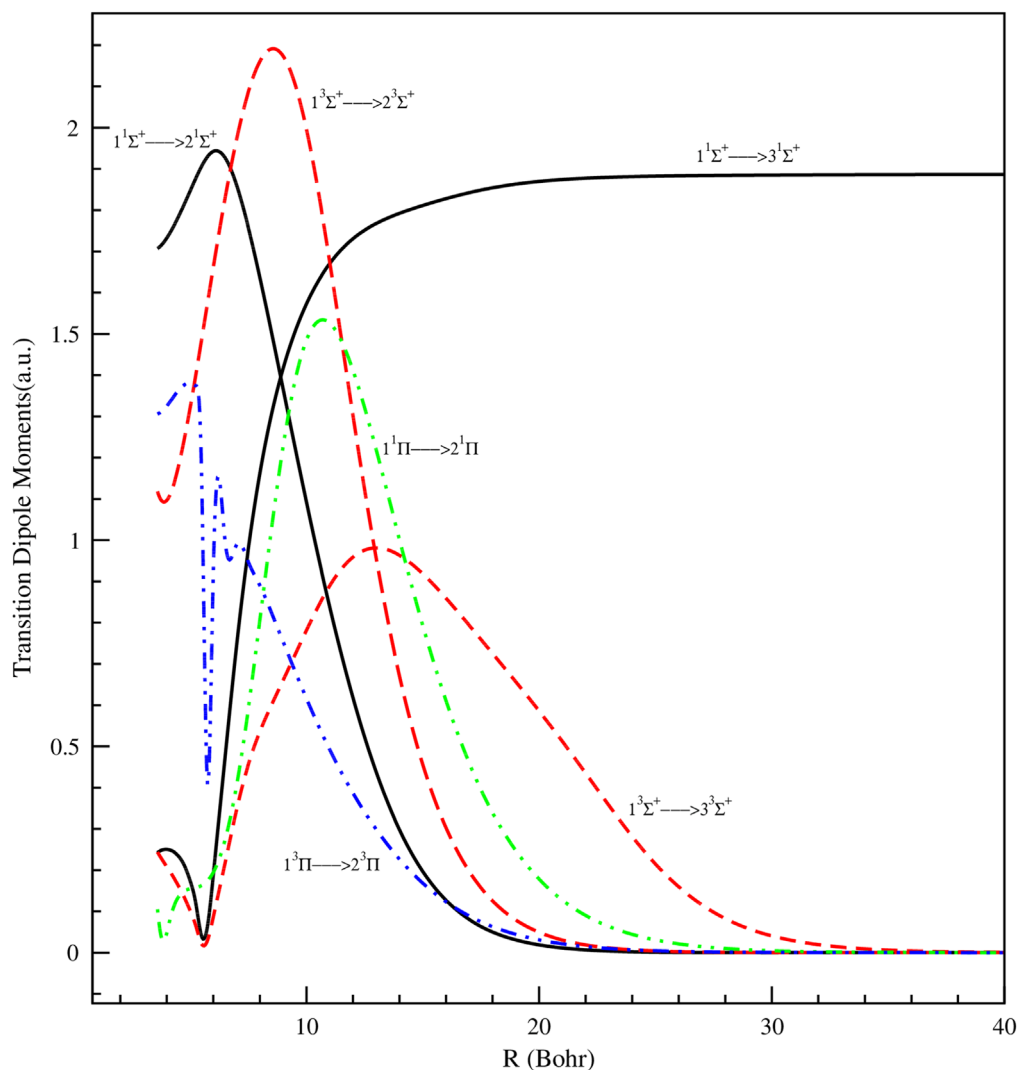


**Figure 8.** Transition dipole moment of the  $1^3\Sigma^+$  and  $1^3\Pi$  electronic states of  $\text{BeNa}^+$  molecular ion.

$\text{Be}^+\text{Alk}$  and  $\text{BeAlk}^+$ , which are both manifestations of sudden changes of the character of the electronic wave functions. Moreover, we get the same observation as for the permanent dipole moments of the  $1^1\Sigma^+$  and  $3^3\Sigma^+$  electronic states. The abrupt changes in the permanent dipole moments are localized at particular distances. They correspond to avoided crossings between neighbour electronic states. At large distances, the ground state,  $X^1\Sigma^+$ , dipole moments are significant and yield linear behavior functions. We remind that these states are dissociating into,  $\text{Be}(2s^2) + \text{Alk}^+$  ( $\text{Alk} = \text{Na}, \text{K}$  and  $\text{Rb}$ ) and a similar behavior is obtained by Fedorov *et al* [26] for  $\text{BeNa}^+$ . The permanent dipole moments for the other states dissociating into  $\text{Be}(2s^2, 2s2p, 2s3s, 2p^2$  and  $2s3p) + \text{Alk}^+$  ( $\text{Alk} = \text{Na}, \text{K}$  and  $\text{Rb}$ ) characterized by a linear divergence at large internuclear distances expressing the increasing distance between the negative body-fixed and the positive  $\text{Alk}^+$  charge. However, for the other states dissociating into  $\text{Be}^+(2s) + \text{Alk}$  ( $\text{Alk} = \text{Na}, \text{K}$  and  $\text{Rb}$ ), they exhibit a significant permanent dipole moment in a particular region and then it vanishes swiftly at large distances. Therefore, these

states are probably not good candidates for cooling of internal degrees of freedom.

The electronic transition dipole moments (TDM) also are of great interest since they are relevant for the possibility of radiative charge exchange for these type of systems [53, 54] or for photoassociation, spontaneous and stimulated emission [37][55]. In addition, the probabilities for induced absorption and spontaneous emissions per unit of time are proportional to the square of the TDM between two chosen states. Also, this physics quantity has been computed previously for many alkaline earth-hydrogen and alkaline earth-alkali molecular ions such as  $\text{BeH}^+$  [20],  $\text{BeLi}^+$  [21],  $\text{MgLi}^+$  [22],  $\text{CaH}^+$  [23],  $\text{SrH}^+$  [24] and  $\text{BaH}^+$  [25] which is very interesting and constitute the first step to illustrate the repartition of charges between states. In our previous work, we presented only the transition dipole moments between the  $1-2^1\Sigma^+$ ,  $1-3^1\Sigma^+$  and  $2-3^1\Sigma^+$  states for  $\text{BeAlk}^+$  ( $\text{Alk} = \text{Na}, \text{K}, \text{Rb}$ ). In this work, the variation of the transition dipole moments between all considerate states of same symmetries are all calculated according to the inter-nuclear distance. We represent in figures 8–10 only the transition dipole moments between  $1-2$

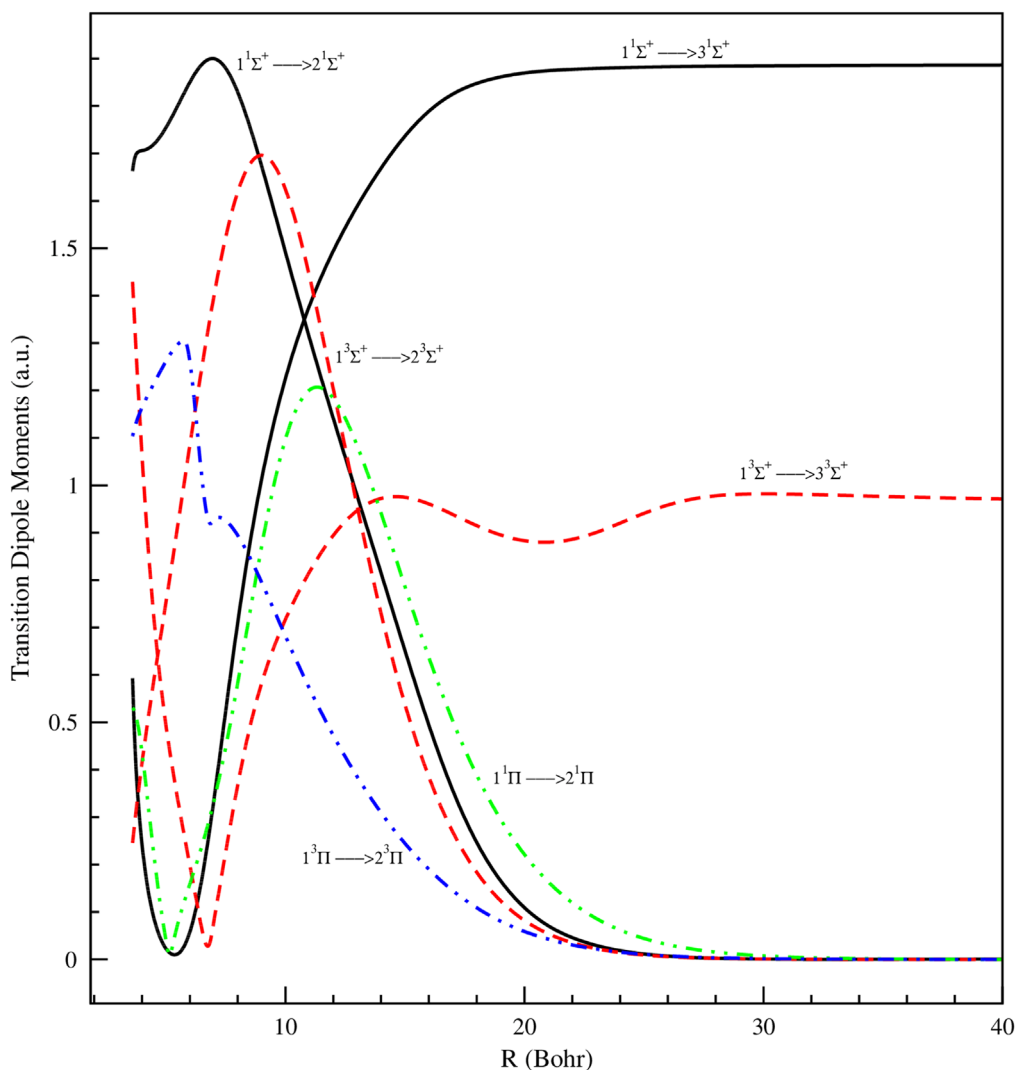


**Figure 9.** Transition dipole moment of the  $1^3\Sigma^+$  and  $1^3\Pi$  electronic states of  $\text{BeK}^+$  molecular ion.

$1^1\Sigma^+$ ,  $1-3^1\Sigma^+$ ,  $1-4^1\Sigma^+$ ,  $1-5^1\Sigma^+$ ,  $1-2^3\Sigma^+$ ,  $1-3^3\Sigma^+$ ,  $1-4^3\Sigma^+$ ,  $1-5^3\Sigma^+$ ,  $1-2^1\Pi$ ,  $1-3^1\Pi$ ,  $1-2^3\Pi$  and  $1-3^3\Pi$  electronic states for each molecular system respectively for  $\text{BeNa}^+$ ,  $\text{BeK}^+$  and  $\text{BeRb}^+$ . Since it becomes increasingly difficult to determine experimentally the dipole moment; thus, our theoretical values become particularly valuable to understand the charge distribution between states. The variations of the dipole moments of adiabatic transitions do not follow a well defined law. These transitions present an interesting behaviour, which has been observed in many previous studies for similar systems (i.e. alkali-alkaline-earth systems) [21, 22, 50]. At short distance, we remark frequent variations which can be related to the avoided crossings. The acuity of the slopes around the node for the dipole is strongly related to the weakness of the avoided crossing for the energy. Quantitatively, the analysis of the curves of the transition dipole moments shows that, the ones between  $1-2^1\Sigma^+$ ,  $1-3^1\Sigma^+$  and  $1-2^3\Sigma^+$  are very large at short distances, when compared to the other transitions. They present maximums located at particular internuclear distances corresponding to an important overlap between the corresponding molecular wave

functions. At larger distances, some transition dipole moments asymptotically reach the corresponding atomic oscillator strength of the allowed atomic transitions. But for ionic-neutral type of transitions, their moment tend to zero, since the continuation wave functions through the dipole moment operator does not allows any covering at large internuclear distance.

### 3.3. Vibrational levels and their radiative lifetimes

**3.3.1. Vibrational levels.** The study of the vibration spectra of diatomic molecules is an area of spectroscopy with a very broad range of applications. In fact, the vibrational spectra of diatomic systems serve as models for polyatomic molecules and it is fundamental to calculate the state for plasmas and stellar atmospheres. For  $\text{BeAlk}^+$  ( $\text{Alk} = \text{Na}, \text{K}$  and  $\text{Rb}$ ) systems, the vibrational levels have been interpolated by least-squares approach. In this work, the vibrational energy levels are obtained using the Numerov method. We have represented in the supplementary materials (S1–S3) is available online at [stacks.iop.org/PS/95/055404/mmedia](https://stacks.iop.org/PS/95/055404/mmedia) the vibrational-level spacing ( $E_{v+1} - E_v$ ) according to

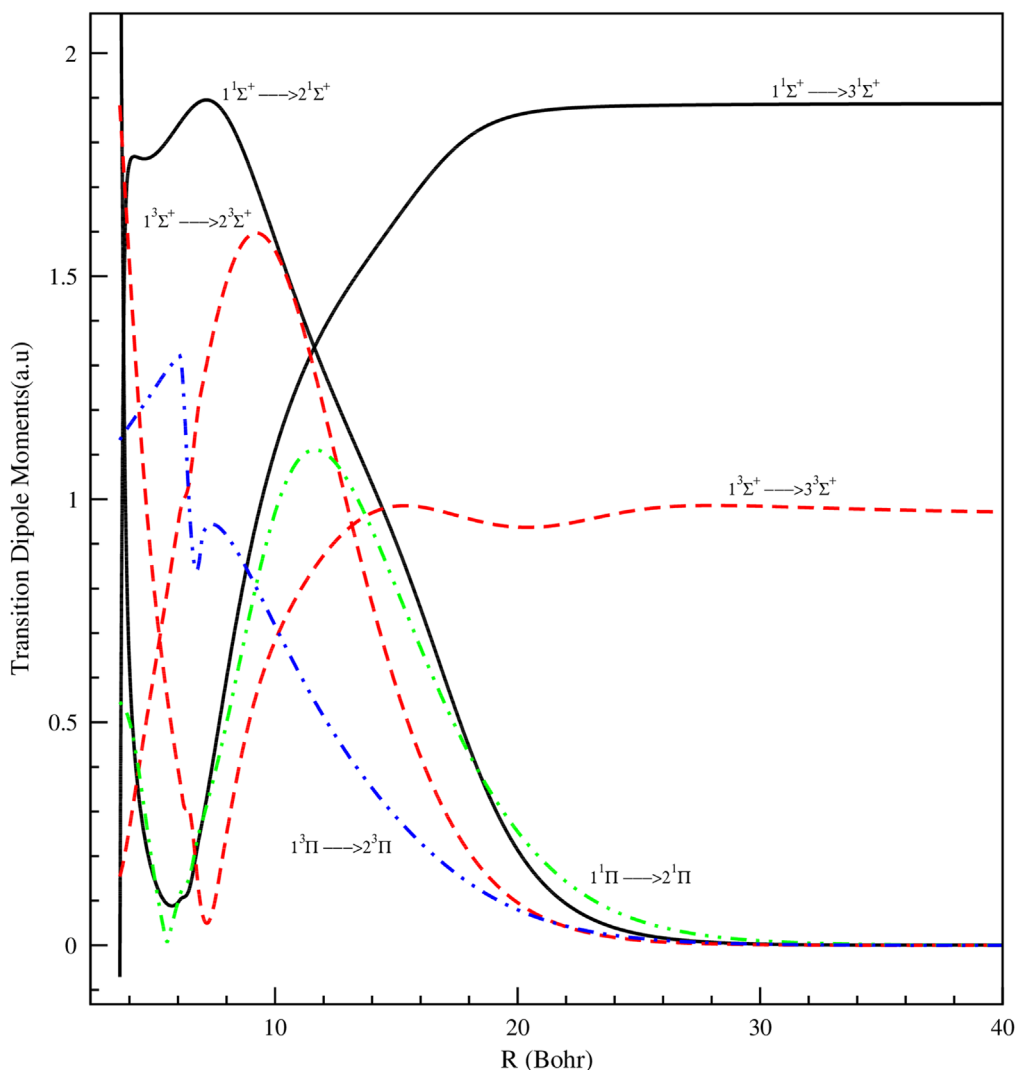


**Figure 10.** Transition dipole moment of the  $1^3\Sigma^+$  and  $1^3\Pi$  electronic states of  $\text{BeRb}^+$  molecular ion.

the vibrational level integer number ‘ $v$ ’ of all the considered  $1^3\Sigma^+$  and  $1^3\Pi$  electronic states for  $\text{BeNa}^+$ ,  $\text{BeK}^+$  and  $\text{BeRb}^+$  systems. In the literature, only Fedorov *et al* [26] have calculated the vibrational energy levels of the ground state for  $\text{BeNa}^+$ . For the reason of comparison, the vibrational-level spacing obtained by Fedorov *et al* [26] is plotted with that obtained in this work in figure 11. The comparison shows a very good agreement. In addition, we calculated the spacing for the higher vibrational level up to 47 for  $\text{BeNa}^+$ . The vibrational levels for the ground state of  $\text{BeK}^+$  and  $\text{BeRb}^+$  are also gathered in figure 11. For the  $X^1\Sigma^+$  ground states, we obtained 47, 46 and 46 vibrational levels respectively for  $\text{BeNa}^+$ ,  $\text{BeK}^+$  and  $\text{BeRb}^+$ . For the first vibrational levels, linear variation of spacing is observed. After that, this behavior becomes slighter and vanishes at  $\text{Be}(2s^2)+\text{Alk}^+$  dissociating limit. Almost all states present strong anharmonic effects and this give rise to a roughly linear behavior, except for the highest levels approaching the dissociation limit, which is followed by a sharper decrease. As usual for ionic systems, the vibrational spacing presents a regular variation dominated by asymptotic behaviors in  $C_4/R^4$ . Due to the

long-range behavior, which has given wide wells for many potential energy curves, several states have trapped large number of vibrational levels. Observing the figures, we note that the vibrational levels of the excited states of  $1^3\Sigma^+$  symmetries are tighter and more numerous than those of the  $1^3\Pi$  states. This confirms the spectroscopic results obtained above, which are interpreted with the importance of the width of the well of potential at the level of the asymptotic limit of  $1^3\Sigma^+$  symmetries states compared with  $1^3\Pi$  states.

**3.3.2. Vibrational lifetimes for the  $X^1\Sigma^+$  ground state.** In the past decade, measurements of the radiative lifetimes of the ground and the highly excited states of alkali alkaline-earth systems have been reported in several works [55, 56][26]. These results would be clearly of interest for physicists working in atomic physics, plasma physics, and astrophysics. In this section, we represent the radiative transition probabilities (Einstein coefficients) and the radiative lifetimes for all vibrational levels of the ground state  $X^1\Sigma^+$  for  $\text{BeAlk}^+$  ( $\text{Alk} = \text{Na}, \text{K}, \text{Rb}$ ) ionic molecules. Using

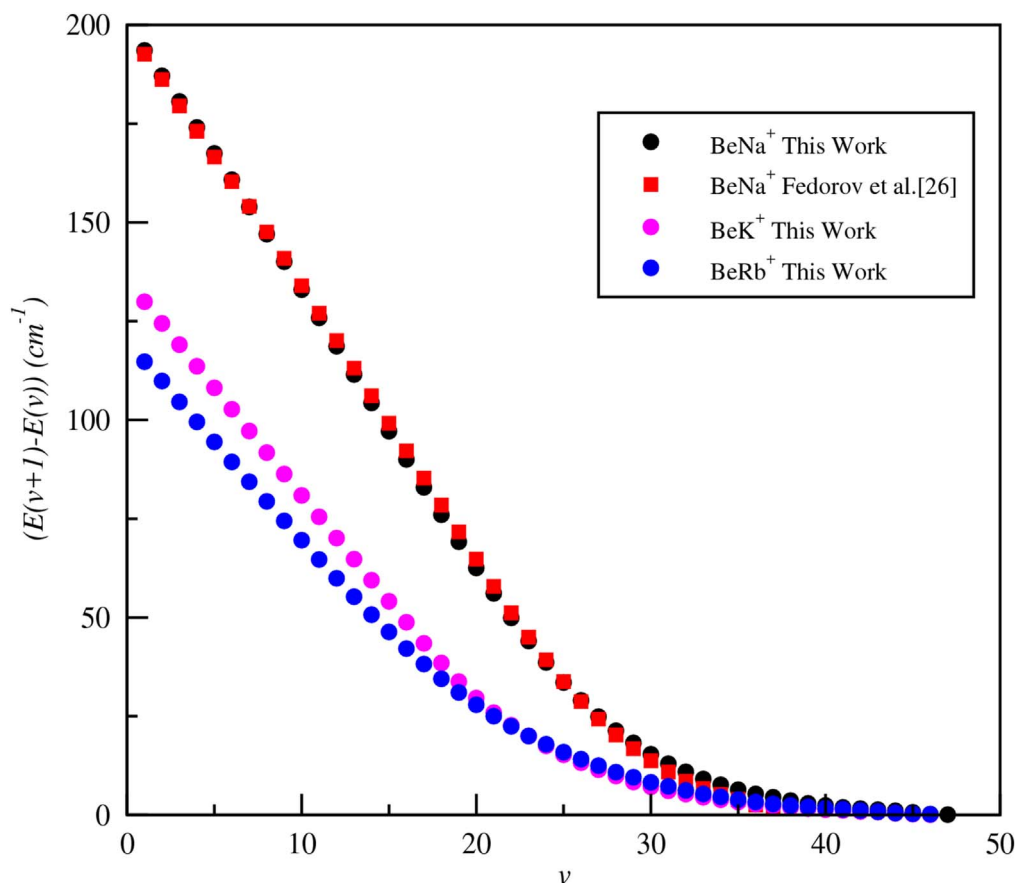


**Figure 11.** Vibrational levels spacing energies of  $X^1\Sigma^+$  electronic states for  $\text{BeAlk}^+$  (Alk = Na, K and Rb).

the ground state potential energy interactions and the permanent dipole moments calculated previously the lifetimes of the vibrational states for the ground state  $X^1\Sigma^+$  of the alkali alkaline-earth ions  $\text{BeAlk}^+$  are evaluated and presented in figure 12. Recently, Fedorov *et al* [26] determined the lifetimes of the ground state vibrational levels for  $\text{BeLi}^+$ ,  $\text{MgLi}^+$ ,  $\text{BeNa}^+$ , and  $\text{MgNa}^+$ , using CCSD(T) and MRCI potential energy curves. For the reason of comparison, the vibrational lifetimes for  $\text{BeNa}^+$  are plotted with that obtained by Fedorov *et al* [26] in figure 12.

Despite the fact that different methods of calculation have been used (FCI with CPP and CCSD (T)), a similar behavior is obtained. This shows the reliability and the accuracy of our calculations and results. In addition, we observed that the lifetime of the ground vibrational state is about two times smaller than that obtained by Fedorov *et al* [26]. Since the vibrational lifetimes of the ground state  $X^1\Sigma^+$ , depend on the permanent dipole moment, the difference between our results and that of Fedorov *et al* [26] is reasonable and could be explained by the difference in the permanent dipole moments due to the use of two different *ab-initio* approaches. For all studied ions ( $\text{BeAlk}^+$ ), the lifetimes of the vibrational states for the ground state  $X^1\Sigma^+$  have an order of magnitude of second and we found that the ground states  $v_X = 0$  vibrational lifetimes are 7.05, 10.12 and 12.36 s for  $\text{BeNa}^+$ ,  $\text{BeK}^+$  and  $\text{BeRb}^+$ , respectively. We notice the same behavior of the lifetime as function of the vibrational

level for all these molecules. Fedorov *et al* [26] observed the same behavior for  $\text{LiBe}^+$ ,  $\text{LiMg}^+$ ,  $\text{NaBe}^+$ , and  $\text{NaMg}^+$ .

As a function of  $v$ , after an initial decay, the lifetime reaches a minimum and then increases reaching values closer, or even larger, than the lifetime of the ground vibrational state  $v = 0$ . This behavior is observed for all three studied molecular ions  $\text{BeAlk}^+$  (Alk = Na, K, Rb). This behavior depends on the dipole moments and the transition frequencies between two levels  $i$  and  $f$ . For the highly excited vibrational states, the transition frequency between levels  $i$  and  $f$ , becomes very small due to the large anharmonicity of the potential energy curve, which is influenced by the increase of the vibrational lifetime. The sum of the Einstein coefficients  $B_{if}$  for stimulated absorption and emission and the sum of the coefficients  $A_{if}$  for spontaneous emission as functions of vibrational state  $i$  for the  $\text{BeNa}^+$  ion are plotted in figure 13. The sum of spontaneous emission  $A_{if}$  for  $\text{BeNa}^+$ ,  $\text{BeK}^+$  and  $\text{BeRb}^+$  are plotted in figure 14. The shortest lifetime corresponds to the peak of the stimulated transition rate and it is close to the maximum of the spontaneous transition rate. It corresponds to  $v = 15$ , 14 and 12 for  $\text{BeNa}^+$ ,  $\text{BeK}^+$  and  $\text{BeRb}^+$ , respectively. For higher vibrational levels, both spontaneous and stimulated rates monotonically decrease because the transition frequencies  $\omega_{if}$  between the highly excited vibrational states become lower because the highly excited states are energetically closer than that of the lower-energy states. Thus, for the highly excited states, the lifetime

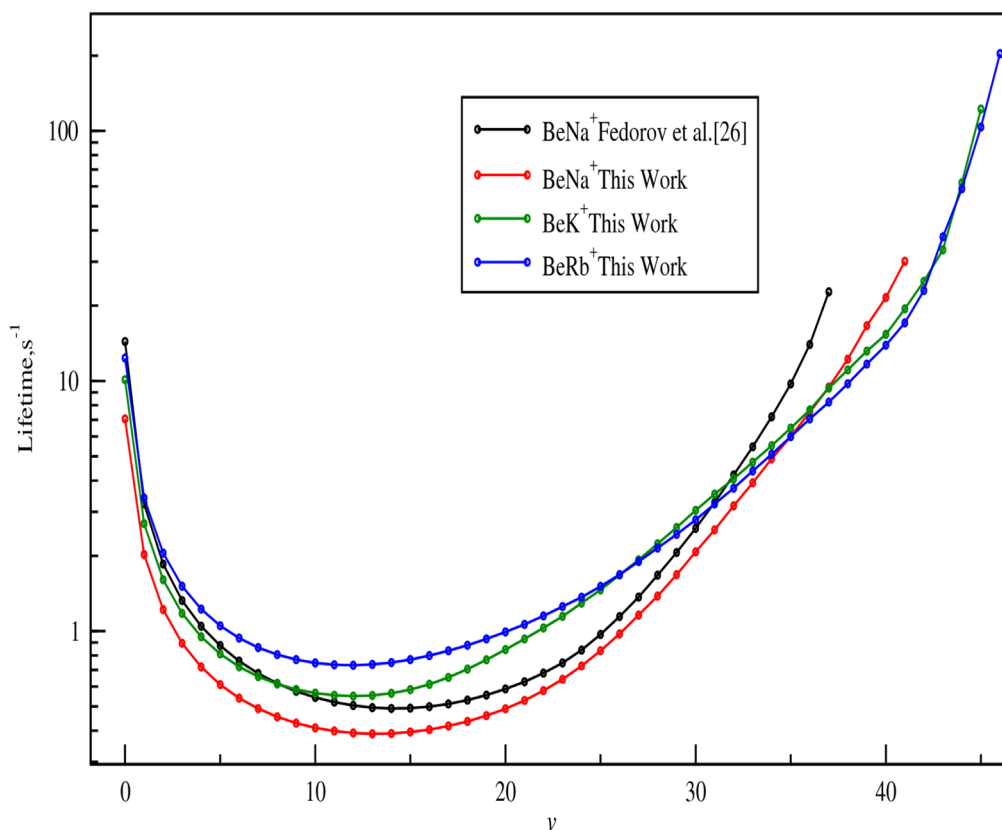


**Figure 12.** Vibrational lifetimes as functions of vibrational level of the ground states compared to that of Fedorov *et al* [26] for  $\text{BeAlk}^+$  (Alk = Na, K and Rb).

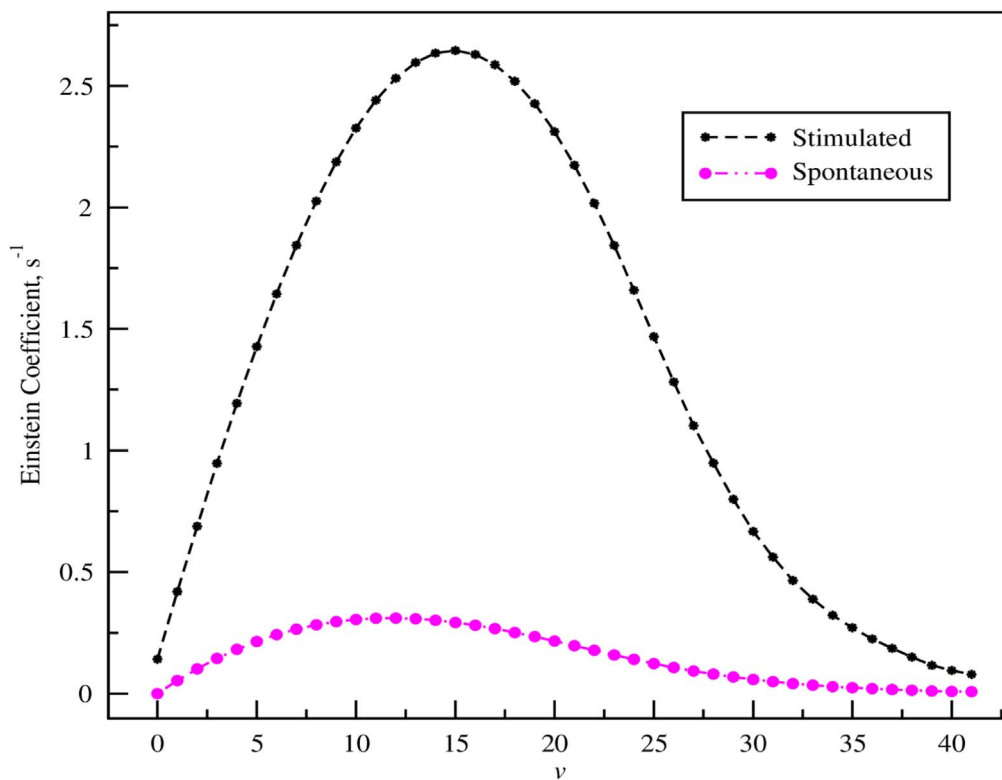


**Figure 13.** Spontaneous (red) and stimulated (black) rates of transitions from  $\text{BeNa}^+$  vibrational states with quantum number.

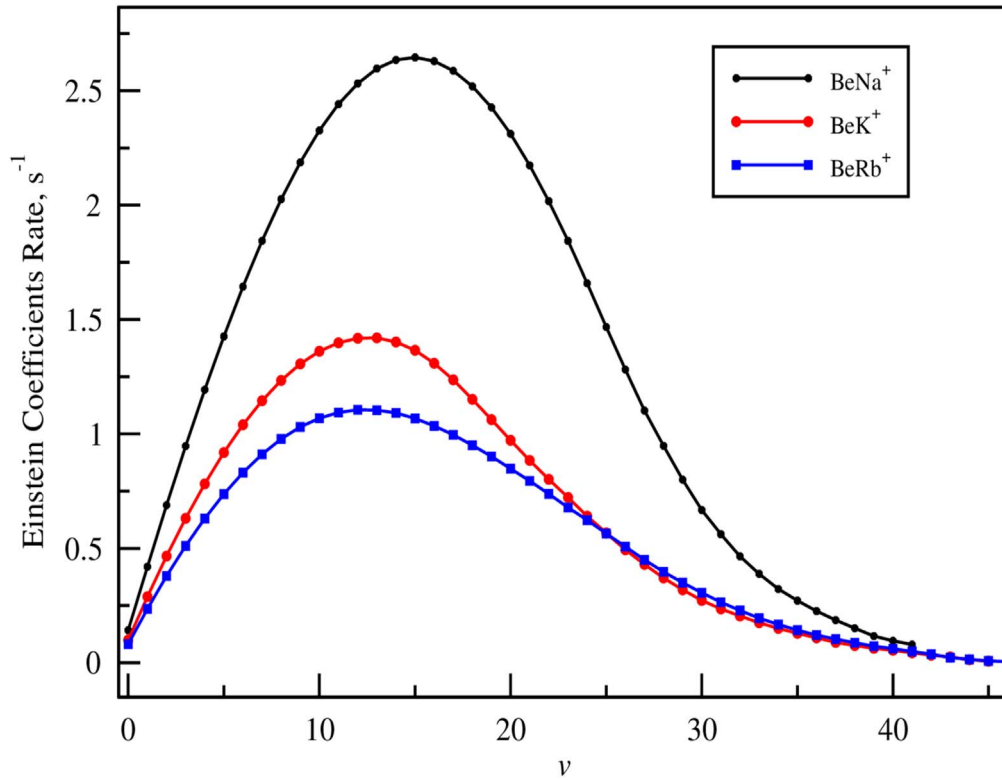


**Figure 14.** The sum of the Einstein coefficients  $A_{if}$  for spontaneous emission as functions of vibrational state  $i$  for the  $\text{BeAlk}^+$  ion ( $\text{Alk} = \text{Na}, \text{K}$  and  $\text{Rb}$ ).

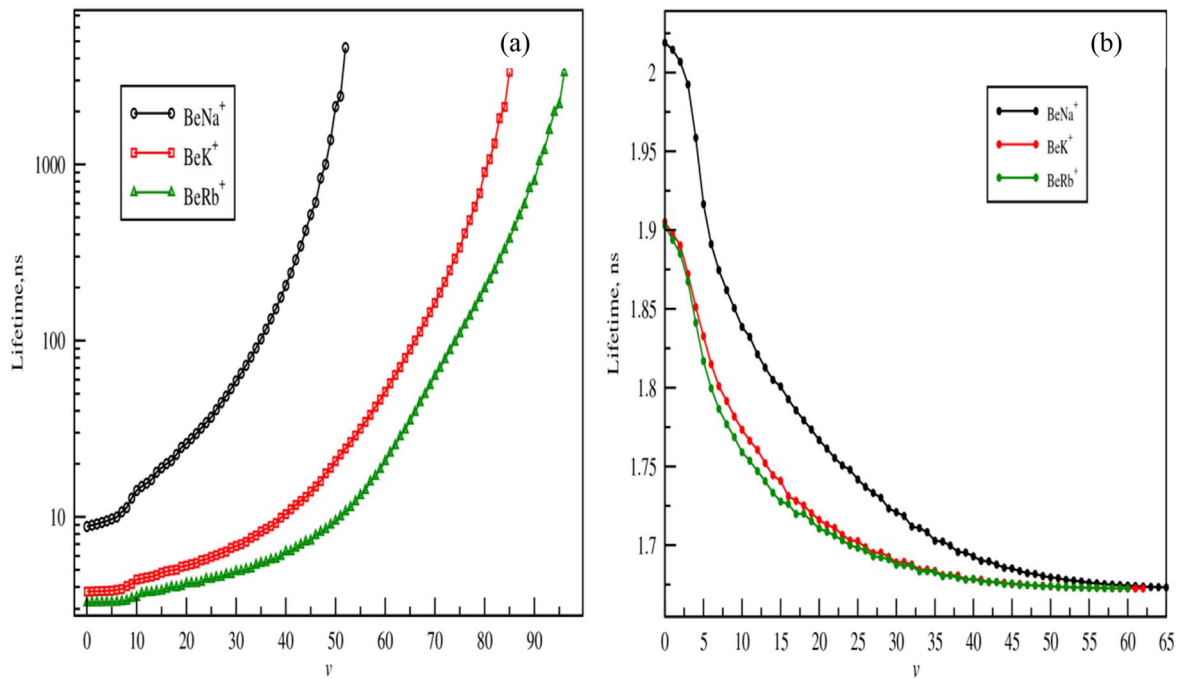


**Figure 15.** Vibrational lifetimes as functions of vibrational level of  $A^1\Sigma^+$  (a) and  $C^1\Sigma^+$  (b) for  $\text{BeAlk}^+$  ( $\text{Alk} = \text{Na}, \text{K}$  and  $\text{Rb}$ ).

increases to reach a value close or even larger, than lifetime of the ground state. This behavior is also observed for the remained studied ions  $\text{BeK}^+$  and  $\text{BeRb}^+$  as represented in figure 14.

**3.3.3. Vibrational lifetimes for the  $A^1\Sigma^+$  and  $C^1\Sigma^+$  states.** In this section, we present the lifetimes of the vibrational states that belong to  $A^1\Sigma^+(2^1\Sigma^+)$  and  $C^1\Sigma^+(3^1\Sigma^+)$  excited states. The total radiative lifetime for  $A^1\Sigma^+$  takes into account the *bound-bound*

and *bound-free* contributions using the two approaches: ‘*Franck-Condon*’ and the ‘*Sum-rule*’ approximations presented in supplementary tables ST1–ST3 respectively for  $\text{BeNa}^+$ ,  $\text{BeK}^+$  and  $\text{BeRb}^+$  molecular ions. We note a very good agreement between the results including the bound-free contribution using the ‘*Franck-Condon*’ approximation and that of ‘*sum-rule*’. This shows that the ‘*Franck-Condon*’ approximation can provide accurate radiative lifetimes even for the higher excited vibrational states where the continuum is larger. To our best knowledge the radiative lifetimes of the vibrational levels of the  $A^1\Sigma^+$  state of the  $\text{BeNa}^+$ ,  $\text{BeK}^+$  and  $\text{BeRb}^+$  molecules are presented here for the first time.

Based on the ‘*Franck-Condon*’ approximation, the vibrational lifetimes of the  $A^1\Sigma^+$  and  $C^1\Sigma^+$  for  $\text{BeNa}^+$ ,  $\text{BeK}^+$  and  $\text{BeRb}^+$  are represented in figure 15. For all molecules, we observe that the radiative lifetimes of the lower vibrational levels of the  $A^1\Sigma^+$  have an order of magnitude of nanosecond. As observed previously for  $\text{NaCa}^+$  [56], the radiative lifetimes of the  $A^1\Sigma^+$  state increases with the vibrational levels and it is found with an order of nanosecond. The radiative lifetimes for  $v' = 0$  are predicted to be 8.81 ns, 3.76 ns and 3.25 ns, respectively for  $\text{BeNa}^+$ ,  $\text{BeK}^+$  and  $\text{BeRb}^+$ .

For all molecules, the radiative lifetimes corresponding to the  $C^1\Sigma^+$  state have also an order of magnitude of nanosecond. For  $v' = 0$  they are predicted to be 2.02 ns, 1.905 ns and 1.902 ns, respectively for  $\text{BeNa}^+$ ,  $\text{BeK}^+$  and  $\text{BeRb}^+$ . As represented in figure 15, the variation of vibrational state lifetimes curves of the  $C^1\Sigma^+$  state descend to reach the same constant corresponding to the pure atomic lifetime of the second excited state ( $^1P^o(2s2p)$ ) of the Be atom of 1.78 ns measured by Fischer *et al* [57]. This value is very close to the calculated radiative lifetime of the last vibrational levels, which is found to be about 1.67 ns.

#### 4. Conclusion

In the present work, an extended and complete study is devoted to the  $\text{BeNa}^+$ ,  $\text{BeK}^+$  and  $\text{BeRb}^+$  molecular ions. We have performed *ab-initio* calculations for the potential energy curves, their related spectroscopic constants, and electric permanent and transition dipole moments for their ground states and nearly 48 low-lying excited states of different symmetries,  $^1,3\Sigma^+$ ,  $^1,3\Pi$  and  $^1,3\Delta$ . The used calculation method is based on a non-empirical pseudo-potential approach for  $\text{Be}^{2+}$ ,  $\text{Na}^+$ ,  $\text{K}^+$  and  $\text{Rb}^+$  cores, which allows treating each ionic molecule as a two-electron system, where full configuration interaction FCI calculations can be easily performed. As it is expected the permanent dipole moments for several electronic states dissociating into  $\text{Be}+\text{Alk}^+$  illustrate a pure linear behavior as a function of internuclear distance  $R$ . For the remaining states dissociating into  $\text{Be}^++\text{Alk}$ , the permanent dipole moment vanishes quickly at large distances. In addition, vibrational energy level spacings and their radiative lifetimes are extensively represented and analyzed in this study. For all molecules, we observe that the radiative lifetimes of the lower vibrational levels of the  $X^1\Sigma^+$  ground state have an order of magnitude of second (s). However, an order of ns is observed for  $A^1\Sigma^+$  and  $C^1\Sigma^+$  vibrational states. Only the permanent and

radiative lifetimes of the ground state of  $\text{BeNa}^+$  have been performed in the past. The comparison between our results and that of the literature shows a very good agreement for  $\text{BeNa}^+$ . For the remaining molecular systems,  $\text{BeK}^+$  and  $\text{BeRb}^+$ , due to the similarity of the theoretical approach, we are confident about the high accuracy of the presented results, which can be faithfully be used in future theoretical and experimental investigations.

#### ORCID iDs

Hamid Berriche  <https://orcid.org/0000-0002-1442-669X>

#### References

- [1] Adams C S and Riis E 1997 Laser cooling and trapping of neutral atoms *Prog. Quant. Electron.* **21** 1–79
- [2] Metcalf H J and Van der Straten P 2007 Laser cooling and trapping of neutral atoms *The Optics Encyclopedia: Basic Foundations and Practical Applications*
- [3] Tomza M, Jachymski K, Gerritsma R, Negretti A, Calarco T, Idziaszek Z and Julienne P S 2019 Cold hybrid ion-atom systems *Rev. Mod. Phys.* **91** 035001
- [4] Adams C S, Sigel M and Mlynek J 1994 Atom optics *Phys. Rep.* **240** 143–210
- [5] Townsend C G, van Druten N J, Andrews M R, Durfee D S, Kurn D M, Mewes M–O and Ketterle W 1996 Bose–Einstein condensation of a weakly interacting gas *OSA Trends in Optics and Photonics (TOPS) Ultracold Atoms and Bose–Einstein Condensation* ed Keith Burnett (Washington, DC: Optical Society of America) vol. 7, pp 2–13
- [6] Birkl G, Kassner S and Walther H 1992 Multiple-shell structures of laser-cooled  $^{24}\text{Mg}^+$  ions in a quadrupole storage ring *Nature. London.* **357** 310–3
- [7] Mitchell T B, Bollinger J J, Dubin D H E, Huang X, Itano W M and Baughman R H 1998 Direct observations of structural phase transitions in planar crystallized ion plasmas *Phys. Plasmas* **282** 1290–3
- [8] Drewsen M, Brodersen C, Hornekær L, Hangst J S and Schiffer J P 1998 Large ion crystals in a linear Paul trap *Phys. Rev. Lett.* **81** 2878–2881
- [9] Cirac J I and Zoller P 1995 ‘Quantum computations with cold trapped ions *Phys. Rev. Lett.* **74** 4091–4
- [10] Koelmeij J C J, Roth B, Wicht A, Ernsting I and Schiller S 2007 Vibrational spectroscopy of HD + with 2-ppb accuracy *Phys. Rev. Lett.* **98** 173002
- [11] Schiller S and Korobov V 2005 Tests of time independence of the electron and nuclear masses with ultracold molecules *Phys. Rev. A* **71** 032505
- [12] Smith I W M 2008 *Low Temperature and Cold Molecules* (London: Imperial College Press)
- [13] Meyer E R, Bohn J L and Deskevich M P 2006 Candidate molecular ions for an electron electric dipole moment experiment *Phys. Rev. A* **73** 062108
- [14] Hall F H J, Aymar M, Bouloufa N, Dulieu O and Willitsch S 2011 Light-assisted ion-neutral reactive processes in the cold regime: radiative molecule formation versus charge exchange *Phys. Rev. Lett.* **107** 243202
- [15] Hall F H, Eberle P, Hegi G, Raoult M, Aymar M, Dulieu O and Willitsch S 2013 Ion-neutral chemistry at ultralow energies: dynamics of reactive collisions between laser-cooled  $\text{Ca}^+$  ions and Rb atoms in an ion-atom hybrid trap *Mol. Phys.* **111** 2020–32
- [16] Hall F H, Aymar M, Raoult M, Dulieu O and Willitsch S 2013 Light-assisted cold chemical reactions of barium ions with rubidium atoms *Mol. Phys.* **111** 1683–90

- [16] Schmid S, Härter A and Denschlag J H 2010 Dynamics of a cold trapped ion in a Bose–Einstein condensate *J Phys. Rev. Lett.* **105** 133202
- [17] Schmid S, Härter A, Frisch A, Hoinka S and Denschlag J H 2012 An apparatus for immersing trapped ions into an ultracold gas of neutral atoms *J. Rev. Sci. Instrum.* **83** 053108
- [18] Idziaszek Z, Calarco T, Julienne P S and Simoni A 2009 Quantum theory of ultracold atom-ion collisions *Phys. Rev. A* **79** 010702
- [19] Foucrault M, Millié Ph and Daudey J P 1992 Nonperturbative method for core–valence correlation in pseudopotential calculations: application to the Rb<sub>2</sub> and Cs<sub>2</sub> molecules *J. Chem. Phys.* **96** 1257–64
- [20] Farjallah M, Ghanmi C and Berriche H 2013 Structure and spectroscopic properties of the beryllium hydride ion BeH<sup>+</sup>: potential energy curves, spectroscopic constants, vibrational levels and permanent dipole moments *Eur. Phys. J. D* **67** 1–16
- [21] Ghanmi C, Farjallah M and Berriche H 2017 Theoretical study of the alkaline-earth (LiBe)<sup>+</sup> ion: structure, spectroscopy and dipole moments *J. Phys. B: At. Mol. Opt. Phys.* **50** 1–9
- [22] ElOualhaziand R and Berriche H 2016 Electronic structure and spectra of the MgLi<sup>+</sup> ionic molecule *J. Phys. Chem. A* **120** 452–65
- [23] Habli H, Dardouri R, Oujia B and Gadéa F X 2011 *Ab-initio* adiabatic and diabatic energies and dipole moments of the CaH<sup>+</sup> molecular ion *J. Phys. Chem.* **115** 14045–53
- [24] Habli H, Mejrissi L, Issaoui N, Yagmour S J, Oujia B and Gadéa F X 2015 ‘*Ab-initio* calculation of the electronic structure of the strontium hydride ion (SrH<sup>+</sup>)’ *Int. J. Quantum Chem.* **115** 172–86
- [25] Szczepkowski J, Grochola A, Kowalczyk P, Dulieu O, Guéroul R, Żuchowski P S and Jastrzebski W 2018 Experimental and theoretical study of the B (2) <sup>2</sup>Σ<sup>+</sup> → X (1) <sup>2</sup>Σ<sup>+</sup> system in the KSr molecule *J. Quant. Spec. Rad. Trans.* **210** 217–24
- [26] Fedorov D A, Barnes D K and Varganov S A 2017 *Ab-initio* calculations of spectroscopic constants and vibrational state lifetimes of diatomic alkali-alkaline-earth cations *J. Chem. Phys.* **147** 124304
- [27] Sumida K, Hill M R, Horike S, Dailly A and Long J R 2009 Synthesis and hydrogen storage properties of Be<sub>12</sub>(OH) 12 (1, 3, 5- benzenetribenzoate) 4 *JACS* **131** 15120–1
- [28] Pospelov M and Pradler J 2011 Primordial beryllium as a big bang calorimeter *Phys. Rev. Lett.* **106** 121305
- [29] Berriche H 2003 Theoretical study of the lowest electronic states of the LiNa<sup>+</sup> molecule *J. Mol. Struct.* **663** 101–8
- [30] Berriche H, Ghanmi C and Ben Ouada H 2005 Theoretical study of the electronic states and transition dipole moments of the LiK<sup>+</sup> molecule *J. Mol. Spect.* **230** 161–7
- [31] Ghanmi C, Berriche H and Ben Ouada H 2006 *Ab-initio* study of NaRb<sup>+</sup>: potential energy curves, spectroscopic constants and atomic polarizabilities *J. Mol. Spect.* **235** 158–65
- [32] Jendoubi I, Berriche H, Ben Ouada H and Gadea F X 2012 Structural and spectroscopic study of the LiRb molecule beyond the born–oppenheimer approximation *J. Phys. Chem. A* **116** 2945–60
- [33] Ghanmi C, Berriche H and Ben Ouada H 2005 Theoretical investigation of the KRb<sup>+</sup> ionic molecule: potential energy, K and Rb polarizabilities and long-range behaviour . *Lect. Ser. Comp. Comput. Scien.* **4** 703–9
- [34] Bouzouita H, Ghanmi C and Berriche H 2006 *Ab-initio* study of the alkali-dimer cation Li<sub>2</sub><sup>+</sup> *J. Mol. Struct.* **777** 75–80
- [35] Ghanmi C, Bouzouita H, Berriche H and Ben Ouada H 2006 Theoretical investigation on CsLi<sup>+</sup> and CsNa<sup>+</sup> ionic molecules *J. Mol. Struct.* **777** 81–6
- [36] Berriche H, Ghanmi C, Farjallah M and Bouzouita H 2008 ‘Theoretical investigation of the alkali-dimer cation K<sub>2</sub><sup>+</sup>: potential energy, dipole moment and atomic polarizabilities’ *J. Comp. Meth. Scien. Eng.* **8** 297–318
- [37] Ladjimi H, Sardar D, Farjallah M, Alharzali N, Naskar S, Mlika R, Berriche H and Deb B 2018 Spectroscopic properties of the molecular ions BeX<sup>+</sup> (X = Na, K, Rb): forming cold molecular ions from an ion–atom mixture by stimulated Raman adiabatic process *Mol. Phys.* **14** 1812–26
- [38] Durand P and Barthelat J C 1975 A theoretical method to determine atomic pseudopotentials for electronic structure calculations of molecules and solids *Theor. Chem. Acta* **38** 283–302.
- [39] Müller W, Flesh J and Meyer W 1984 ‘Treatment of intershell correlation effects in *ab-initio* calculations by use of core polarization potentials. Method and application to alkali and alkaline earth atoms’ *J. Chem. Phys.* **80** 3297–310
- [40] Foucrault M, Millie P and Daudey J P 1992 Nonperturbative method for core–valence correlation in pseudopotential calculations: application to the Rb<sub>2</sub> and Cs<sub>2</sub> molecules *J. Chem. Phys.* **96** 1257–64
- [41] Berriche H 2003 ‘Theoretical study of the lowest electronic states of the LiNa<sup>+</sup> molecule’ *J. Mol. Struct.* **663** 101–8
- [42] Magnier S and Millie P 1996 Potential curves for the ground and numerous highly excited electronic states of K<sub>2</sub> and NaK *Phys. Rev. A* **54** 204–18
- [43] Pavolini D, Gustavsson T, Spiegelmann F and Daudey J P 1989 Theoretical study of the excited states of the heavier alkali dimers. I. The RbCs molecule ,*J. Phys. B.* **22** 1721–31
- [44] Moore C E 1989 *Atomic Energy Levels, NSRDS-NBS No. 467* (Washington, DC: US Government Printing Office)
- [45] Zemke W T, Crooks J B and Stwalley W C 1978 Radiative and nonradiative lifetimes for vibrational levels of the A<sup>1</sup>Σ<sup>+</sup> state of <sup>7</sup>LiH *J. Chem. Phys.* **68** 4628–30
- [46] Partridge H and Langhoff S R 1981 Theoretical treatment of the X<sup>1</sup>Σ<sup>+</sup>, A<sup>1</sup>Σ<sup>+</sup>, and B<sup>1</sup>Π states of LiH *J. Chem. Phys.* **74** 2361–71
- [47] Mabrouk N and Berriche H 2017 ‘Theoretical evaluation of the radiative lifetimes of LiCs and NaCs in the A<sup>1</sup>Σ<sup>+</sup> state’ *Russ. J. Phys. Chem. A* **91** 1474–85
- [48] Stolyarov A V and Pupyshv V I 1994 ‘Approximate sum rule for diatomic vibronic states’ *Phys. Rev. A* **49** 1693–7
- [49] Pazyuk E A, Stolyarov A V and Pupyshv V I 1994 Approximate sum rule for diatomic vibronic states as a tool for the evaluation of molecular properties *Chem. Phys. Lett.* **228** 219–24
- [50] Pyykkö P 1989 ‘*Ab-initio* study of bonding trends among the 14-electron diatomic systems: from B<sub>2</sub><sup>+</sup> to F<sub>2</sub><sup>+</sup>’ *Mol. Phys.* **67** 871–8
- [51] Staunum P F, Hojbjerg K, Skyt P S, Hansen A K and Drewsen M 2010 Rotational laser cooling of vibrationally and translationally cold molecular ions *Nat. Phys.* **6** 271–4
- [52] Schneider T, Roth B, Duncker H, Ernsting I and Schiller S 2010 All-optical preparation of molecular ions in the rovibrational ground state *Nat. Phys.* **6** 275–8
- [53] Idziaszek Z, Calarco T, Julienne P S and Simoni A 2009 Quantum theory of ultracold atom-ion collisions *Phys. Rev. A* **79** 010702
- [54] Makarov O P, Côté R, Michels H and Smith W W 2003 Radiative charge-transfer lifetime of the excited state of NaCa<sup>+</sup> *Phys. Rev. A* **67** 67042705
- [55] Aymar M, Guéroul R and Dulieu O 2011 Structure of the alkali-metal-atom + strontium molecular ions: towards photoassociation and formation of cold molecular ions *J. Chem. Phys.* **135** 0643051–11
- [56] Gacesa M, Montgomery J A, Harvey Michels H Jr and Coté R 2016 Production of NaCa<sup>+</sup> molecular ions in the ground state from cold atom-ion mixtures by photoassociation via an intermediate state *Phys. Rev. A* **94** 013407
- [57] Fischer cf and Tachiev G 2004 Breit–pauli energy levels, lifetimes, and transition probabilities for the beryllium-like to neon-like sequences *Atom. Data Nucl. Data* **1**–184